ISPRS Journal of Photogrammetry and Remote Sensing 178 (2021) 219–239

Contents lists available at ScienceDirect

ISPRS Journal of Photogrammetry and Remote Sensing

journal homepage: www.elsevier.com/locate/isprsjprs

Wood and leaf separation from terrestrial LiDAR point clouds based on mode points evolution

Zhenyang Hui [a,b], Shuanggen Jin [b,c], Yuanping Xia [a], Leyang Wang [a], Yao Yevenyo Ziggah [d], Penggen Cheng [a,*]

[a] Faculty of Geomatics, East China University of Technology, Nanchang 330013, China
[b] School of Remote Sensing and Geomatics Engineering, Nanjing University of Information Science and Technology, Nanjing 210044, China
[c] Shanghai Astronomical Observatory, Chinese Academy of Sciences, Shanghai 200030, China
[d] Faculty of Mineral Resources Technology, University of Mines and Technology, Tarkwa, Ghana

ARTICLE INFO

Keywords:
Terrestrial LiDAR point clouds
Wood and leaf separation
Mean shift
Mode points
Evolution

ABSTRACT

To improve the accuracy of wood and leaf points classification for individual tree, this paper proposed a separation method based on mode points evolution from terrestrial LiDAR point clouds. In the proposed method, the Mean Shift method was used to first acquire the mode points, which were then adopted as nodes to build a network graph for the individual tree. By path retracing and calculating the visiting frequency of each node, the wood seed nodes were detected. To obtain more wood nodes, the wood seed nodes were evolved based on three constraints, namely the shortest path length of the evolved nodes to the base node should be smaller, the evolved nodes should not belong to the leaf nodes that have been detected by path retracing and the verticality of the evolved nodes should be similar as the wood seed nodes. After wood nodes evolution, the segments corresponding to each wood seed node were merged together to obtain the final wood points. The proposed method has been evaluated using nine tree samples with seven different tree species. Experimental results showed that the proposed method can achieve an average wood and leaf classification accuracy of 0.892. The average F1 score for wood was 0.871, while the average F1 score for leaf was 0.900. Compared to two other famous wood and leaf classification methods, the proposed method can achieve better classification results.

1. Introduction

Light detection and ranging (LiDAR) has been developing very fast in the past decades (Vosselman and Maas, 2010). Based on different platforms, LiDAR systems can be separated into three groups, namely airborne LiDAR, terrestrial LiDAR and handheld LiDAR. The terrestrial LiDAR is a ground-based LiDAR system, which can emit laser pulses actively to obtain the three-dimensional coordinate information of the target objects (Wang et al., 2020). Compared with other measurements, terrestrial LiDAR can provide dense point clouds rapidly and accurately (Liang et al., 2018). Thus, terrestrial LiDAR has been widely used for forest inventories, such as forest parameter calculation (Henning and Radtke, 2006; Cote et al., 2011; Olofsson et al., 2014), biomass estimation (Kankare et al., 2013; Yu et al., 2013; Wang et al., 2019), and leaf area estimation (Beland et al., 2011; Li et al., 2017), etc.

For most forest applications using terrestrial LiDAR system, the separation of wood and leaf is a perquisite (Xi et al., 2018; Moorthy et al., 2020). For instance, it is necessary to first extract the leaf points when calculating the leaf area. This is because the existence of wood components will overestimate the leaf area index around 3% to 32% (Zhu et al., 2018). Moreover, when estimating wood volumes or above ground biomass, the leaf points will influence the estimated results (Calders et al., 2015). Therefore, wood and leaf should be correctly separated before carrying out the follow-up applications. However, the separation of wood and leaf is still a challenging task to achieve due to the existence of different tree structures or species. Especially for complex trees, it is generally hard to make a clear difference between wood and leaf points.

This paper proposed a wood and leaf classification method based on mode points evolution. In the proposed method, the mode points that represent the segment results are first acquired using the Mean Shift method. In this way, the point-wise classification is transformed into the

* Corresponding author.
E-mail addresses: huizhenyang2008@ecut.edu.cn (Z. Hui), sgjin@shao.ac.cn (S. Jin), ypxia@ecut.edu.cn (Y. Xia), wleyang@ecut.edu.cn (L. Wang), yyziggah@umat.edu.gh (Y. Yevenyo Ziggah), pgcheng@ecut.edu.cn (P. Cheng).

https://doi.org/10.1016/j.isprsjprs.2021.06.012
Received 6 November 2020; Received in revised form 1 May 2021; Accepted 15 June 2021

segment-wise classification. Thus, the computation burden is relieved and the implementation efficiency is improved. Based on the path retracing and the path frequency detection, the leaf nodes and wood seed nodes are detected. In order to evolve the wood seed nodes, three major constraints were considered. Firstly, the shortest path length of the evolved nodes to the base node should be smaller. Secondly, the evolved nodes should not belong to the leaf nodes that have been detected by path retracing, and finally the verticality of the evolved nodes should be similar as the wood seed nodes. By merging the segments corresponding to all the wood nodes, the final wood points are obtained. The proposed wood and leaf separation method is easy to implement and achieves good classification performance, which will provide a good foundation for the forest inventory applications using terrestrial LiDAR.

1.1. Related works

In the past decade, many famous wood and leaf separation methods have been proposed. According to different separation principles, these methods can be classified into three categories, namely geometric features based, radiometric features based and the graph based methods.

The geometric features based methods mainly classify wood and leaf points based on their different geometric features. In general, the leaf points show "scatter" properties, while the wood points show "linear" or "surface" properties. These three geometric salient features can be calculated according to the covariance matrix of neighboring points (Moorthy et al., 2020; Vicari et al., 2019). Thus, many researchers have proposed supervised or unsupervised learning methods for the classification by means of Support Vector Machine (SVM), Random Forest (RF), or Gauss Mixture Model (GMM) (Brodu and Lague, 2012; Ma et al., 2016; Xi et al., 2020). For example, Wang et al. (2017) tested the performance of four famous machine learning methods, including SVM, RF, GMM and Naive Bayes (NB). Experimental results showed that the RF classifier achieved the best wood and leaf classification result (Wang et al., 2017). However, the study conducted by Wang et al. (2017) was based on two isolated trees. Further test on more tree species and more complicated forest environments should be conducted to show the effectiveness of the machine learning methods. One famous salient feature-based supervised learning method was developed by Ma et al. (2016). In their method, three salient features were calculated for each point based on the covariance matrix. Then the GMM was utilized for separating photosynthetic and nonphotosynthetic components (Ma et al., 2016). Experimental results indicate that the local dimensional features can separate leaves and stems effectively. However, in this method the radius of locating neighboring points is determined experimentally. In effect, the optimal determination of the neighboring radius is still unresolved. To avoid setting the neighboring radius, Moorthy et al. (2020) proposed a multi-scale supervised learning method. Instead of setting the neighboring radius as a fix constant, this method calculated the salient features using varying neighbor sizes (Moorthy et al., 2020). In this way, features of different scales can be obtained. Experimental results show that the multi-scale supervised learning methods can achieve better wood and leaf separation results. Although the multi-scale supervised learning methods performed better than the single-scale methods, the approach is computationally expensive and time consuming. To solve this problem, Zhou et al. (2019) proposed a multi-optimal-scale method. In their method, several candidate scales were first specified. Hereafter, the Shannon entropy for each scale is calculated using the principal component analysis (PCA). The first m scales with smallest eigen-entropies are selected as the optimal scales. Compared to the multi-scale method, the multi-optimal-scale method can achieve more stable separation accuracy with several limited optimal scales (Zhou et al., 2019). Moreover, the multi-optimal-scale method can relief the computation burden and save computation time.

In addition to these point-wise separation methods, some researchers have tried to calculate the geometric features of the segments to achieve better leaf and wood separation results. Wan et al. (2020) first applied the connected component segmentation to the plot-level tree points. Two kinds of geometric features, including the salient features and the distance between the centroid of each segment to the ground were calculated to identify the wood segments (Wan et al., 2020). Similarly, Zhang et al. (2019) also adopted the connected component segmentation method. Here, the geometric features for each segment, including the number of points within the segment and the height-to-width ratio of the segment were calculated. The segments with larger number of points and higher height-to-width ratio were determined as the stem segments (Zhang et al., 2019). Compared with the point-wise classification methods, the segment-wise classification methods can generally reduce the computational burden and uncertainties of classification results (Zhang et al., 2013; Zhang et al., 2019). Ferrara et al. (2018) applied the segmentation strategy to separate the photosynthetic and non-photosynthetic components. In their method, the point clouds were first partitioned into voxels, which were further classified as active and non-active voxels based on the number of points within the voxel. Subsequently, the Density-Based Spatial Clustering of Applications with Noise (DBSCAN) method was applied to these voxels. The most highly populated cluster is classified as wood-cluster. Although a promising wood-leaf separation results can be achieved, the performance of this method is still influenced by fine-tuning two parameters in the DBSCAN clustering method, namely the radius *Eps* and the minimum number of points within the *Eps*-neighborhood (Ferrara et al., 2018).

In general, the machine learning methods based on the geometric features can produce satisfactory wood and leaf classification results. However, the performance of the machine learning methods is affected by three factors, namely the classifier, the training samples and the calculated features. Thus, the generalization capability of the machine learning methods becomes limited, especially when applying to some unknown scenes. Moreover, the machine learning methods always involve huge computational burden, which will be time consuming. Comparing with the point-wise classification using the machine learning method, the segment-wise classification methods can reduce the computational burden and uncertainties of the point clouds classification. However, the wood and leaf classification results heavily depend on the segmentation results. That is, if the classification results exist errors, the performance of wood and leaf classification cannot be good.

In addition to the geometric features, such as linear features, surface features and scatter features, as adopted in the machine learning methods, some researches have tried to combine some radiometric features to test the effectiveness of the combination of these two kinds of features (Penasa et al., 2014). The radiometric features, especially the intensity values have been proved to be useful in many classification works (Penasa et al., 2014; Lin and Herold, 2016; Zhang and Liu, 2016). Zhu et al. (2018) adopted seven radiometric features and six geometric features for the separation. The radiometric features were mainly involved with intensity and RGB information, while the geometric features were mainly calculated using eigenvalues and heights for each point. Zhu et al. (2018) indicated that combining the geometric and intensity features, the three classes including ground, wood and foliage can be better identified. By calculating the importance of the features using the RF function, Zhu et al. (2018) concluded that the geometric features were more important than the radiometric features. Windrim and Bryson (2020) developed a new point-based deep learning architecture for stem segmentation, which feed the intensity information into the learning representation. Experimental results indicated that the voxel-based deep learning method that used the intensity information of each point performed the best. Windrim and Bryson (2020) also concluded that incorporating the intensity values into a method will result in higher segmentation accuracy (Windrim and Bryson, 2020). However, the deep learning method is always device-dependent. Compared with Central Processing Unit (CPU), the implementation on a Graphics Processing Unit (GPU) enables to process much more dense point clouds.

The reflected laser intensity is generally affected by the target reflectance, incidence angle and the distance between the laser scanner and the target (Fang et al., 2015; Tan and Cheng, 2016; Xu et al., 2017). To obtain accurate intensity values, the influence of incidence angle and distance should be modified. Tan et al. (2021) corrected the intensity values using the polynomial model (Tan and Cheng, 2015), which was followed by applying the k-means clustering method to obtain two classified categories, including leaf points and the mixture of the leaf and wood points. Subsequently, the k-means clustering algorithm was adopted to refine the wood points since the leaf points are generally sparser. Experiments by Tan et al. (2021) also indicated that combining the intensity and geometric information for constraints could achieve promising classification results. Hackenberg et al. (2015) mentioned that the albedo of woods is different from that of leaves. Thus, the leaf points can be separated from wood points by setting the intensity threshold. Three different intensity thresholds (125, 150 and 175) were tested by Hackenberg et al. (2015). It was found that the higher the threshold value the more leaf points were removed, meanwhile, parts of the wood points will also be wrongly deleted. However, the appropriate intensity threshold should be set by visual inspection. In addition to using intensity information, some researchers try to adopt reflected echo information for the wood and leaf separation (Yao et al., 2011; Yang et al., 2013; Danson et al., 2014). Danson et al. (2014) and (2018) have tried to use the terrestrial LiDAR with the dual-wavelength full-waveform function to describe the forest canopy. In their works, it was demonstrated that this technology can accurately describe the forest structure. Similarly, Li et al. (2013) also found that the dual-wavelength terrestrial LiDAR has the potential to discriminate leaf points from wood points. Zhao et al. (2011) discriminated the woody structures from the foliage by calculating the ratio of total power of the reflected pulse and its width. This was because the trunks and branches are solid targets. Thus, they generally produce a sharply peaked return pulse.

In general, combining the geometric and the radiometric features can provide more information to discriminate wood points from leaf points leading to better classification outputs. The intensity information has been proved to be effective. However, the intensity values need to be corrected since the reflection intensity is not only related to the target material, but also related to the pulse travelling distance and reflection angle. Although the full-waveform data has shown the potential in separating the leaves and woods, not all LiDAR systems can provide this kind of data.

Another kind of wood and leaf classification methods is the graph-based. The graph-based methods are based on a principle that the tree points can be arranged as a connected topological network. By applying the shortest path analysis the wood or larger branches can be separated from the leaves. The graph structure has been successfully applied in the tree crown extraction (Strimbu and Strimbu, 2015; Dong et al., 2020). In the graph, nodes and edges are included (Livny et al., 2010). Generally, the nodes correspond to the points while the edge weights are the distances between each two points. Wang et al. (2020) proposed a recursive point cloud segmentation method called LeWoS by setting three constraints to prune several edges. By exercising this graph segmentation technique recursively, a robust segmentation result was achieved (Wang et al., 2020). According to different geometric features of the segments, including linearity and size, wood and leaf points can be separated. To obtain a spatial smooth classification result, a class regularization technique is also applied. The advantage of this method is that the LeWoS is a fully automatic tool with only one parameter required to be set. Thus, this method can be easily and universally applied to the LiDAR point clouds obtained from any forest type. Vicari et al. (2019) proposed a wood and leaf separation algorithm based on geometric features and structural analysis. In their method, four different algorithms were adopted. Two methods were based on the point-wise geometric features. By separating the GMMs, point clouds were classified into a predefined number of classes. The other two methods were based on the shortest path detection with the tree assumed as a network. By applying the shortest path analysis, the paths with higher frequency of occurrence are detected as trunk of branches (Vicari et al., 2019). The strength of this method is that adopting four different methods together will ensure improvement in the robustness and generalization of the method thereby achieving better classification accuracy and stability. Tao et al. (2015) also applied the shortest path analysis for detecting wood points. In their method, point clouds were first sliced into bins. By detecting geometric primitives (such as circles or line segments) and applying shortest path analysis, the skeleton wood points can be obtained. In terms of the broad-leaved trees, the proposed method can achieve good classification accuracy with larger branches extracted effectively. However, some tiny twigs shaded by leaf clusters could be wrongly classified as leaves.

The graph-based methods are easy to implement. Conversely, when encountering large number of points the constructed network will undertake huge computational burden. In the shortest path analysis, although the path retracing method performs well in detecting stems or larger branches, some small branches especially some tiny twigs close to the leaves are easily misclassified. In terms of the path frequency detection method, although this method can detect finer branching structures, many stem points are misclassified as leaf points since their occurrence frequency in the graph structure are not high. How to improve the stem points detection accuracy while keeping a finer branching structure is still challenging.

1.2. Contributions of this work

Although many works on wood and leaf separation have been proposed, there are still some unresolved challenges:

i Most existing works cannot obtain a finer branching structure, especially when encountering complex tree structures, some tiny twigs are easily misclassified as leaf points.

ii The omission or commission errors are uniformly distributed in the wood and leaf classification results, which can greatly affect forest applications, such as tree modeling or photosynthesis analysis.

iii The existing works cannot obtain a stable and accurate wood-leaf classification accuracy towards different tree species. The robustness and generalization of the wood and leaf classification method need to be improved.

To solve these problems, this paper proposed a separation method based on mode points evolution. On the whole, the proposed method can be seen as a hybrid model, which combines the strengths of the graph-based and the geometric features based methods. To most graph-based methods, no matter the path retracing algorithm or the path frequency detection algorithm adopted, this kind of methods cannot obtain a finer branching structure while keeping a higher stem points extraction accuracy. In this paper, both the path retracing algorithm and the path frequency detection algorithm are combined for detecting leaf and wood nodes, respectively. Moreover, the method named as “evolution” was proposed in this paper. In the process of modes evolution, the geometric feature, namely verticality is adopted for recovering the misclassified stem points and tiny twig points. It is important to note that the geometric feature applied in this paper was only used for optimizing the separation results by the graph-based method which is different from the machine learning based geometric features methods, (e.g. multi-optimal-scale method proposed by Zhou et al. (2019)). In the proposed mode points evolution method, Mean Shift was adopted for the segmentation to obtain the mode points that were used to build the graph structure. Although the methods proposed by Ferrara et al. (2018), Wan et al. (2020) and Tan et al. (2021) all used certain clustering algorithms for segmenting the tree points, their wood-leaf separation principles are totally different from what the present authors have proposed. For instance, Ferrara et al. (2018) applied the DBSCAN clustering algorithm to the active voxels to obtain the wood-cluster directly since the grouped wood voxels are general larger. Wan et al. (2020) proposed a segment-wise geometric features calculation method. Tan

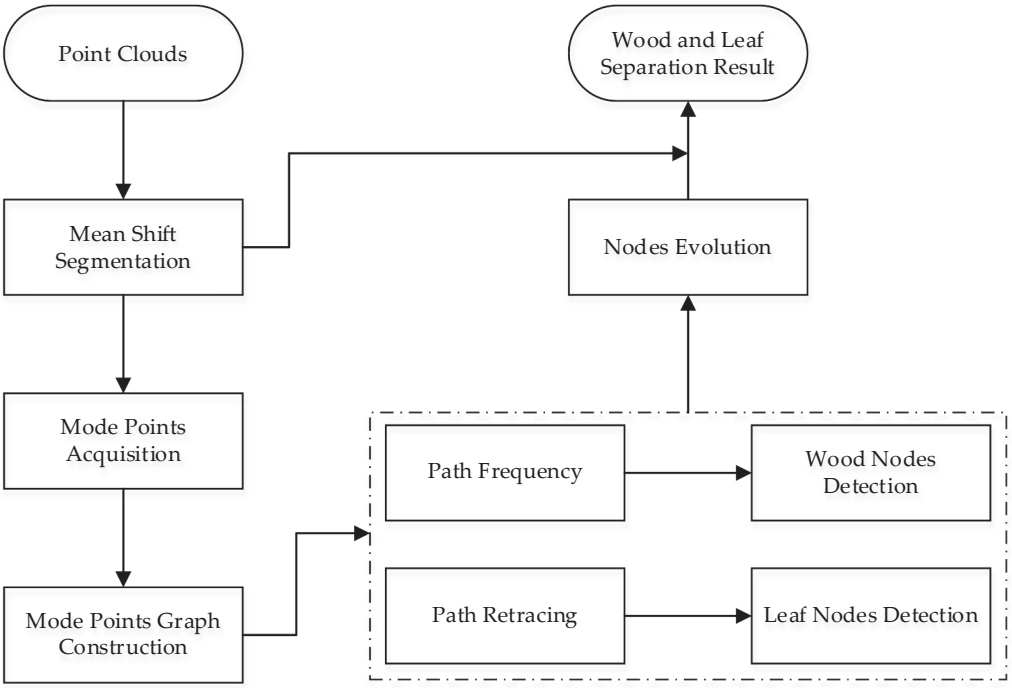

Fig. 1. Flowchart of the proposed method.

et al. (2021) applied k-means clustering method to the corrected intensity data and density data subsequently to separate the wood from leaf points. Yet, the proposed method mainly applied the Mean Shift method for obtaining mode points, which will be served as nodes in the graph construction. In so doing, the constructed graph will not be complicated and the shortest path analysis to the graph will not be time-consuming.

Overall, the main contributions of the proposed method are as follows:

- A hybrid wood-leaf separation model was developed, which combines the strength of graph-based and geometric features based methods. The hybrid model can reduce uncertainties of wood-leaf classification results and improve the separation accuracy towards different tree species and structures.
- A method named as "Modes Points Evolution" was proposed. The mode points with similar verticality were evolved as the same labels. In so doing, the misclassified wood points can be recovered and a finer branching structure can be obtained.
- Mean Shift segmentation algorithm was applied to obtain the mode points that were served as nodes in the graph construction. Using the mode points instead of tree points as the nodes, the constructed graph will be less complicated. The following shortest path analysis to the graph will be efficient.
- The commute-time distance that refers to the path length in the graph was proposed. Compared to Euclidean distance, the commute-time distance can better reflect the position relation between nodes. In so doing, the "Evolution" can be conducted accurately and the wood points can be detected accurately.

2. Methodology

In this paper, the mode points play a critical role in the process of obtaining wood points. The method named as "Mode Points Evolution" was proposed for obtaining higher wood points detection accuracy and finer branching structure. Here, "Evolution" has a similar meaning as "Growing". It means that the detected wood modes points are evolving and dynamic rather than fix and static. The flowchart of the proposed method is shown in Fig. 1.

From Fig. 1, it can be found that the Mean Shift segmentation method is first applied to the point clouds. The clustering center of each segment is the mode point. Then, the mode points are utilized to construct a graph, which is the main structure for detecting wood and leaf points. According to the constructed graph, all the mode points will be connected as a network. In the network graph, the nodes are the mode points, while the weighted edges are the distances between each two mode points.

According to the constructed graph, the wood nodes are detected based on path frequency, while the leaf nodes are detected by path retracing. In so doing, the proposed method can combine the strengths of path frequency detection and path retracing. In general, the detected wood and leaf nodes are not complete. To reduce the omission error, nodes evolution is applied to achieve better wood and leaf nodes detection results. According to the Mean Shift segmentation results, each node corresponds to a segment. Thus, the final wood and leaf points separation results can be acquired by merging the corresponding Mean Shift segments.

The proposed method mainly concludes the following four steps: i Mode points acquisition by the Mean Shift segmentation, ii Graph construction and shortest path analysis, iii Leaf nodes detection based on pass retracing and nodes evolution, and iv Wood nodes detection based on path frequency and nodes evolution. The steps will be described in detail in the following subsections.

2.1. Mode points acquisition by mean shift segmentation

As mentioned above, mode points play a key role in the wood points acquisition. Here, the advantages of using the mode points instead of each point in point clouds are twofold. On the one hand, the mode points represent the segmentation results of the point clouds. Thus, the point-wise wood and leaf separation can be transformed into a segment-wise separation approach. Obviously, the implementation efficiency can be improved. On the other hand, using the huge point clouds to build the graph is hard to realize. Conversely, using the mode points will relief the

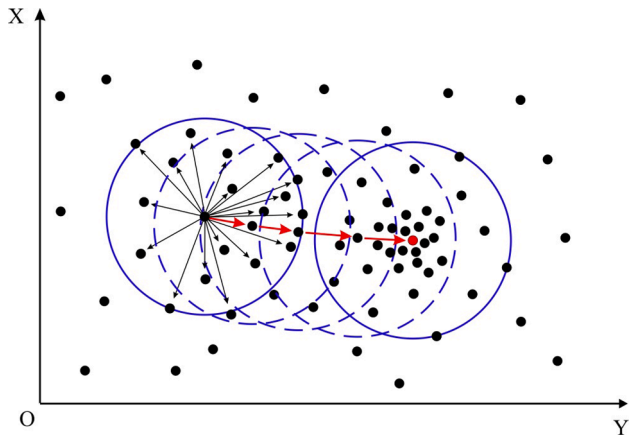

Fig. 2. Mean Shift clustering process.

computation burden greatly.

The mode points can be obtained using the Mean Shift method. Mean Shift is a non-parametric clustering method (Cheng, 1995). Compared to the traditional K-means method, Mean Shift does not need to preset the number of clusters. Thus, Mean Shift is generally used in the clustering or segmentation for unknown scenes. As shown in Fig. 2, Mean Shift is an iterated method. In each iteration, the mean shift vector is calculated first as the red arrow shown in Fig. 2. The mean shift vector generally points to the direction in which the probability density increases. Thus, after several iterations, the point will be shifted to a mode point as the red point shown in Fig. 2. The points sharing the same or similar mode point will be clustered together.

The mean shift vector is defined as Eq. (1) (Dai et al., 2018).

$$Meanshift_h(V_p) = \frac{\sum_{i=1}^{n} V_i \cdot G\left(\left\|\frac{V_p - V_i}{h}\right\|^2\right)}{\sum_{i=1}^{n} G\left(\left\|\frac{V_p - V_i}{h}\right\|^2\right)} - V_p \tag{1}$$

where $Meanshift_h(V_p)$ represents the mean shift vector. For three-dimensional point clouds, V_p is equal to the three coordinates of point p. n is the number of neighboring points of point, which is determined by the bandwidth h. $G(\cdot)$ is the Gaussian function. Specially, when $\left\|\frac{V_p - V_i}{h}\right\|$ is greater than 1, $G(\cdot)$ is equal to zero. Thus, the bandwidth h will influence the clustering results (Hu et al., 2017). A larger h will lead to more points clustered together. Consequently, the results may be under-segmentation. On the contrary, a smaller h will lead to over-segmentation. In this study, the Mean Shift method is adopted to segment the trunk or branches into sections. Thus, the bandwidth h generally needs to be larger than diameter of the trunk. In general, $h \in [0.3, 1.0]$ is appropriate in this study.

Fig. 3 shows the process of mode points acquisition. Fig. 3 (a) is the raw point clouds of an individual tree. Fig. 3 (b) shows the Mean Shift segmentation results. From Fig. 3 (b), it can be found that the trunk or branches are segmented into sections, while leaf points segmented into small clusters. For the Mean Shift segments, the mode points are kept. Finally, the individual tree can be represented by the mode points as shown in Fig. 3 (c).

2.2. Graph construction and shortest path analysis

When the mode points are acquired, these mode points can be used to construct the graph. Compared with the methods using all the points as the nodes, the proposed method is obviously fast, easy to implement and computational burden reduced. The graph is composed of nodes and edges, which can be represented as $Graph = (Node, Edge)$. As mentioned above, the nodes are the mode points in this paper. Obviously, each two nodes will have an edge. To make the graph less complicated, this paper made the following constraint as Eq. (2).

$$Edge(p_i, p_j) = \begin{cases} dis(p_i, p_j), & if \quad dis(p_i, p_j) \leqslant r \\ false, & otherwise \end{cases} \tag{2}$$

where $Edge(p_i, p_j)$ is the edge between nodes p_i and p_j, $dis(p_i, p_j)$ is the Euclidean distance between the two nodes, r is the constraint radius. Eq. (2) means that if p_j is the neighbor of p_i within the radius r, the edge between nodes p_i and p_j is existed. Moreover, the edge weight is equal to

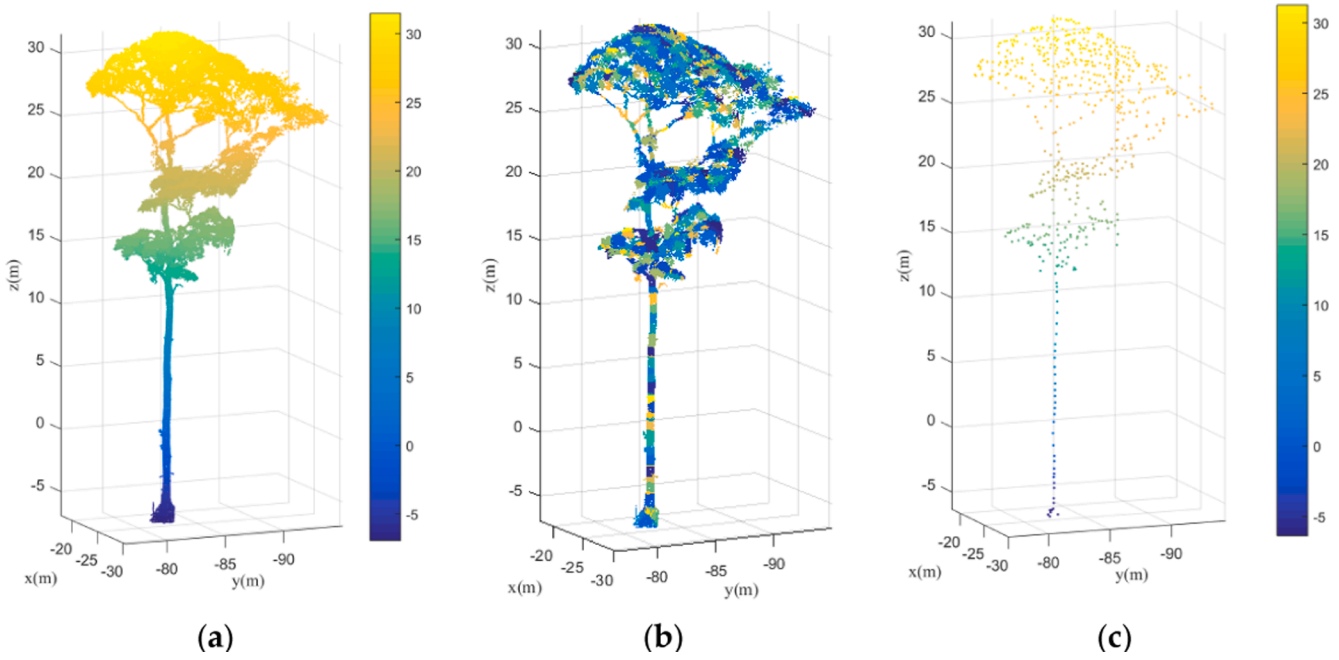

Fig. 3. The process of mode points acquisition. (**a**) The raw point clouds colored based on elevation; (**b**) Mean Shift segmentation results with each segmentation randomly colored; (**c**) The mode points colored based on elevation.

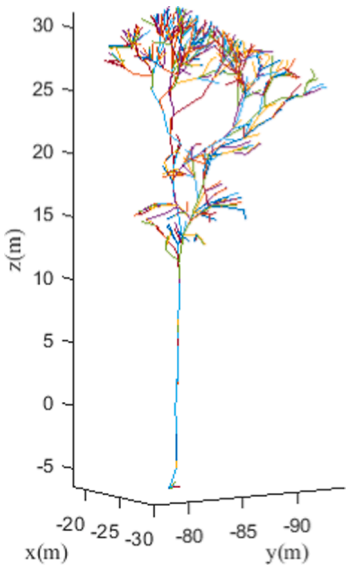

Fig. 4. Shortest paths of all the nodes to the base node.

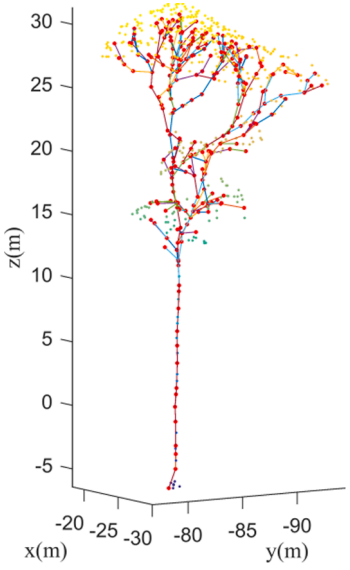

Fig. 5. The result of path retracing. The red points are the nodes that the paths passing through, while the other points are the other nodes in the graph. (For interpretation of the references to colour in this figure legend, the reader is referred to the web version of this article.)

the Euclidean distance between the two nodes. If $dis\left(p_i, p_j\right)$ is larger than r, $Edge\left(p_i, p_j\right)$ is non-existed. Obviously, the radius r will influence the graph construction. If r is smaller, the connected components in the graph will be less, which will make it difficult to conduct the following shortest path analysis. However, the radius r cannot be set too large. If r is too large, the graph will be complicated. The process of generating the graph will be time-consuming. In this paper, r can be set between 1.5 m and 2 m experimentally. The influence of the radius r will be discussed in the following Discussion section.

When the graph is constructed, shortest path analysis can be conducted for each node to the base node. The base node is set as the mode point with the lowest elevation. In other words, the base node represents the tree root, while the other nodes represent trunks, branches or leaves. Since the graph is general connected, each node will have a shortest path to the base node. The shortest path is composed of several nodes that the

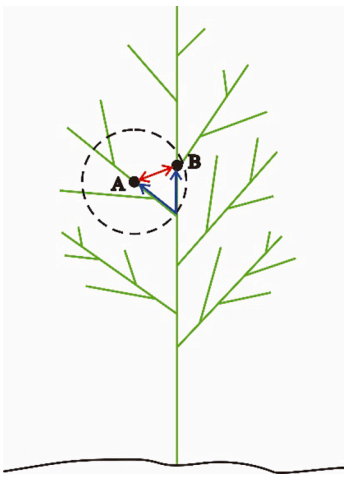

Fig. 6. The comparison of Euclidean distance and commute-time distance between nodes A and B. The red line represents the Euclidean distance, while the blue line represents the commute-time distance. (For interpretation of the references to colour in this figure legend, the reader is referred to the web version of this article.)

end node must pass to the base node. This process can be expressed as Eq. (3).

$$SP(Graph, base, p_m) = \{p_m, p_n, \cdots, base\} \tag{3}$$

where $SP(\cdot)$ represents the shortest path, *Graph* is the constructed graph, *base* is the base node, p_m is the end node, p_n is the node the shortest path must be passed. This paper applied the famous Dijkstra's algorithm to obtain the shortest paths. Fig. 4 shows the shortest paths of each node in Fig. 3 (c) to the base node. Note that Fig. 4 is not the graph structure of the nodes. Fig. 4 shows the shortest paths of all the nodes to the base node. Although there are many paths from the end node to the base node, only the shortest paths obtained using the Dijkstra's algorithm are shown in Fig. 4. That's why the leaf nodes are not connected in the graph. From Fig. 4, it can be found that the shortest paths can basically reflect the tree structure.

2.3. Leaf nodes detection based on pass retracing and nodes evolution

As shown in Fig. 4, the leaf nodes are general at the extremities of each path. According to this characteristic, some leaf nodes can be detected by pass retracing. In this paper, pass retracing means removing successive nodes from the end node towards the base node. The removed nodes are determined by the retracing steps. Since the leaf nodes are general the end node, this paper just needs to retrace one step for each path. For instance, after one step path retracing, the shortest path for the node p_m in Eq. (3) will be $\{p_n, \cdots, base\}$. In other words, the end node $\{p_m\}$ is removed.

The shortest paths in Fig. 4 after path retracing are shown in Fig. 5. It can be found that the leaf nodes at the extremities are excluded in the paths successfully. However, some nodes that are not at the extremities are also not concluded in the paths. It is because the shortest path is trying to find the shortest way to the base node. Some nodes may not be visited. To detect accurate leaf nodes, the nodes that are not at the extremities must be discriminated. It should be noted that the path retracing adopted in this paper tries to detect the leaf nodes at the extremities. Thus, when all the non-leaf nodes that are not at the extremities are detected, the remaining nodes can be seen as the leaf nodes at the extremities.

Considering the fact that the leaf nodes always have larger path length, the nodes that are not visited can be evolved as non-leaf nodes if their path lengths to the base node are smaller than the ones of the nodes on the paths (such as the red points in Fig. 5). In this paper, the nodes

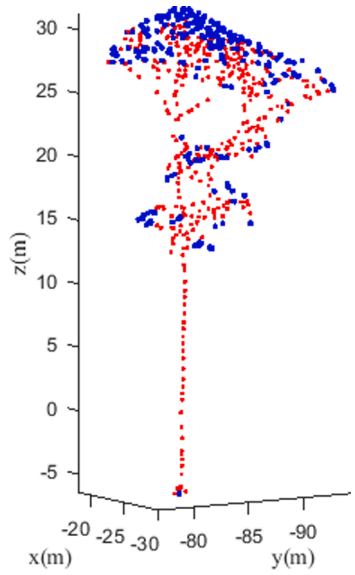

Fig. 7. Leaf nodes detection by seed nodes evolution. The red nodes represent non-leaf nodes. The blue nodes are leaf nodes. (For interpretation of the references to colour in this figure legend, the reader is referred to the web version of this article.)

that the paths passing through are called as seed nodes. For each seed node p^i_{seed}, its neighboring nodes are first located according to Eq. (4).

$$\begin{cases} neighbors_{p^i_{seed}} = \{p_j | ctd(p_i, p_j) \leqslant D, j = 1, 2, \cdots, n\} \\ ctd(p_i, p_j) = SPL(p_i, p_j) \end{cases} \tag{4}$$

$$SPL(p_i, p_j) = \sum SP(Graph, p_i, p_j) \cdot weights \tag{5}$$

where p_j is the node in the graph, n is the number of nodes in the graph, $ctd(p_i, p_j)$ is the commute-time distance between nodes p_i and p_j, which can be calculated according to the shortest path as Eq. (5). Here, *weights* is the edge weight between each two nodes in the path. D is the neighboring distance. In this paper, D is set to 1.5 m.

Note that here the commute-time distance instead of Euclidean distance is calculated between nodes. The commute-time distance is proposed in this paper is because that the commute-time distance can better reflect the position relation between nodes. Fig. 6 is a sketch map of the tree structure, which is formed by a series of nodes. In other words, any point on the tree can be seen as a node. As shown in Fig. 6, "A" and "B" are two nodes. The red line between "A" and "B" represents the Euclidean distance, which can be calculated based on the three-dimensional coordinates of "A" and "B" directly. The blue line represents the commute-time distance between "A" and "B", which can be calculated according to Eq. (5). It is because that the commute-time distance refers to the path length. The node "A"must pass some other nodes to reach node "B". Since the node evolution mentioned in this paper tries to evolve the nodes on the same path, such as the nodes on the same branch or on the same trunk, the nodes on different paths should not be considered as the neighboring nodes. For instance, in Fig. 6, node "B" will be one neighbor of node "A" if the Euclidean distance is considered. Yet, if commute-time distance is selected, node "B" will not be in the neighborhood of node "A". Obviously, the latter is right since node "A" and node "B" are on the different branches.

When the neighbors of each seed node are found, the evolution can be conducted to each seed node. If the node p_i meets the following conditions, p_i will be evolved as a non-leaf node. This can be expressed as Eq. (6).

$$\begin{cases} p_i \in \{Non - leaf\}, & if \quad SP(Graph, base, p_i) \leqslant SP(Graph, base, p^i_{seed}) \\ & \qquad p_i \in neighbors_{p^i_{seed}} \\ p_i \in \{Leaf\}, otherwise \end{cases} \tag{6}$$

where $SP(Graph, base, p_i) \leqslant SP(Graph, base, p^i_{seed})$ means the path length of p_i is smaller than that of the seed node p^i_{seed}. Since p^i_{seed} is a non-leaf node, p_i will also be a non-leaf node. After the nodes evolution based on Eq. (6), all the nodes with shorter path lengths than the ones of seed nodes will be evolved as non-leaf nodes. As shown in Fig. 7, all the evolved non-leaf nodes are colored in red. By contrast, the left nodes (the blue

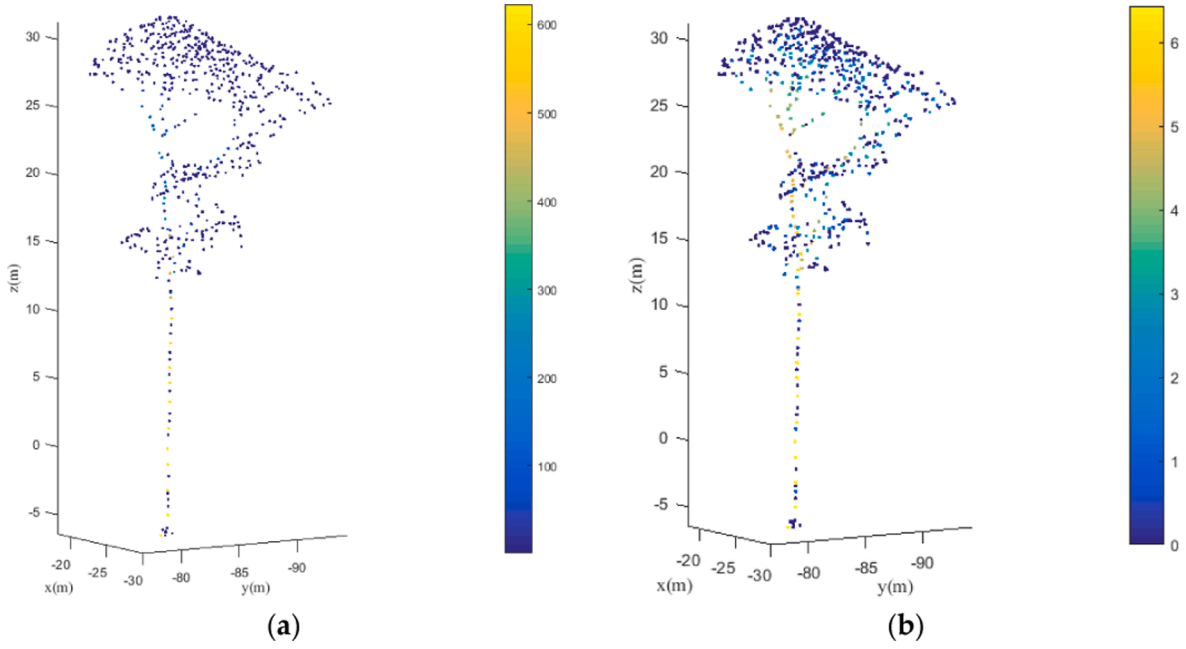

Fig. 8. Tree mode points colored by node visiting frequency. (**a**) The nodes visiting frequency without calculating logarithm; (**b**) The nodes visiting frequency with calculating logarithm.

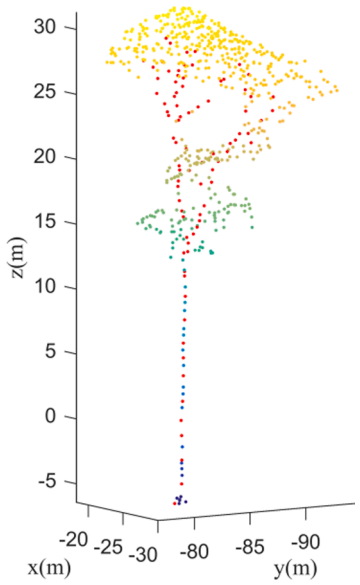

Fig. 9. Wood nodes detection based on node visiting frequency. The red points are the detected wood nodes. (For interpretation of the references to colour in this figure legend, the reader is referred to the web version of this article.)

Table 1
Steps of wood nodes evolution.

Input:	Wood seed nodes p_i, $p_i \in \{Wood\}$, $i = 1, 2, \cdots, m$ Verticality threshold η
Step 1:	Calculate the neighboring nodes ($neighbors_{p_i}$) of wood seed node p_i according to Eq. (4).
Step 2:	For each node $p_j \in neighbors_{p_i}$, calculate its shortest path length $SPL\left(base, p_j\right)$ according to Eq. (5) and calculate its verticality $Verticality\left(p_j\right)$ according to Eqs. (9) and (10).
Step 3:	Evolution constraints: $SPL\left(base, p_j\right) \leqslant SPL(base, p_i) \&\&$ $p_j \notin \{Leaf\} \&\&$ $abs\left(abs\left(Verticality\left(p_j\right)\right) - abs(Verticality(p_i))\right) \leqslant \eta$
Step 4:	If Yes, $\{Wood\} = \{Wood\} \cup \left\{p_j\right\}$.
Output:	Final wood nodes $\{Wood\}$

nodes in Fig. 7) can be detected as leaf nodes. From Fig. 7, it can be found that after evolution the leaf nodes at the extremities are detected successfully. It should be noted that the leaf nodes detected here are not all the leaf nodes in the graph.

2.4. Wood nodes detection based on path frequency and nodes evolution

As shown in Fig. 4, every node has a shortest path to the base node. Each path contains the nodes that the path passing through as listed in Eq. (3). All the paths will contain the nodes that have been visited. Obviously, the nodes at the trunk or branches have a higher visiting frequency. It is because that most paths must pass these nodes to reach the base node. On the contrary, the leaf nodes will have a lower visiting frequency. As shown in Fig. 8 (a), the tree mode points are colored according to the nodes visiting frequency. It can be found that some nodes may be visited more than 600 times, while some nodes may be just visited only once. To narrow down the range of visiting frequency, this paper calculates the logarithm of the frequency. The result is shown in Fig. 8 (b). It is easy to find that the comparison of visiting frequency of different nodes is more distinct. The nodes at the trunk or branches generally have a larger visiting frequency, while the nodes at the extremities generally have a smaller visiting frequency. However, it can also be found that some nodes at the trunk also have a smaller visiting frequency. Some nodes are not even visited. It is because that the short path tries to find a way to the base node with a smallest path length. Thus, some nodes may not be passed. That's why wood nodes should be further evolved to acquire the final wood detection results.

As mentioned above, the nodes with higher visiting frequency are the wood nodes. It can be expressed as Eq. (7).

$$\{Wood\} = \left\{p_i \middle| log\left(f_{p_i}\right) \geqslant \delta \cdot max(log(f)), i = 1, 2, \cdots, n\right\} \tag{7}$$

where f_{p_i} is the times of node p_i has been visited, $max(log(f))$ means the maximum of the logarithm of the nodes visiting times, n is the number of the nodes. δ is a constant, which determines the wood nodes detection result. A smaller δ will lead to more nodes to be detected as wood nodes, while a larger δ will lead to fewer nodes to be detected as wood nodes. In this paper, δ is set to 0.5. The influence of this parameter to the wood nodes detection will be discussed in the Discussion section.

According to Eq. (7), the wood nodes detection results are shown in Fig. 9. It can be found that the nodes on the trunk or branches (red points in Fig. 9) are detected successfully. However, not all the wood nodes are recognized. The omission error for wood detection is large. This paper conducts wood nodes evolution to reduce the omission error.

In this paper, the wood nodes detected by Eq. (7) are named as wood seed nodes. In the process of wood evolution, the evolved wood nodes should meet the following three conditions: i the path length of the evolved wood node to the base node should be smaller than that of the wood seed node; ii the node should not belong to the leaf nodes which have been detected in Section 2.3 (Eq. (6)); iii the verticality of the nodes should be similar, which can be expressed as Eq. (8).

$$abs\left(abs\left(Verticality\left(p_j\right)\right) - abs(Verticality(p_i))\right) \leqslant \eta \tag{8}$$

where $abs()$ means the absolute value, $Verticality()$ is the verticality of the node, and η is the verticality threshold, which determines the evolution condition. In this paper, η is set to 0.125. The influence of verticality threshold η will be discussed in the following Discussion section.

The condition i is based on a principle that the leaf nodes always have a longer path distance to based node than that of wood nodes. In other words, if p_j is one neighbor of the wood seed node p_i, p_j will be evolved as a wood node only if $SPL\left(base, p_j\right)$ is smaller than $SPL(base, p_i)$. The condition ii limits the range of evolution. When the leaf nodes detected in Section 2.3 have been reached the evolution will be stopped. The condition iii set the basic rule for evolution. That is the verticality of the evolved wood node should be similar to the wood seed node. It is because that only the nodes on the same trunk or branch can be evolved. The verticality of each node can be calculated according to Eq. (9).

$$\begin{cases} Verticality(p_i) = normal^z(p_i) \\ normal(p_i) = Vector_{\lambda_3}^{p_i} \end{cases} \tag{9}$$

where $normal^z(p_i)$ is the z component of normal vector $normal(p_i)$. The normal vector can be calculated as the eigen-vector corresponding to the smallest eigenvalue λ_3. The eigen-vectors and eigenvalues can be calculated using the principal component analysis (PCA) by constructing a covariance matrix as Eq. (10).

$$Cov(p_i) = \sum_{i=1}^{n} (p_i - \overline{p})(p_i - \overline{p})^T / n \tag{10}$$

where $\overline{p}$ is the center of the neighboring points of p_i. n is the number of neighboring points. In this paper, n is set to 10. The steps of wood nodes evolution are described in Table 1. Note that wood nodes evolution run only once. After evolution, the wood nodes can be detected successfully as shown in Fig. 10 (a). From Fig. 10 (a), it can be found that most

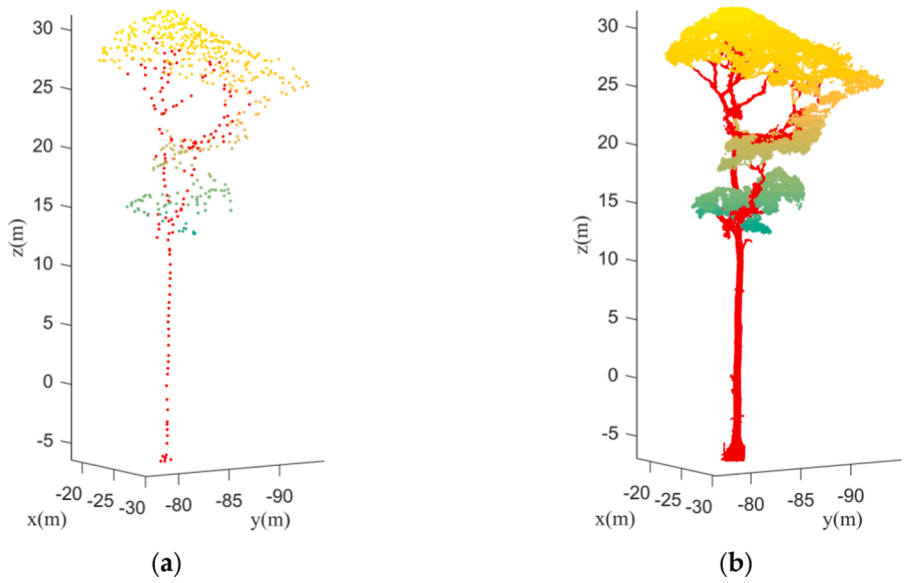

Fig. 10. The detected wood nodes and final separated wood points. (**a**) The wood nodes after evolution; (**b**) The final separated wood points. The red points are wood points, while the other leaf points are colored according to elevation. (For interpretation of the references to colour in this figure legend, the reader is referred to the web version of this article.)

Table 2
Validation data description.

Tree samples	Tree species	Region	Scanner	Tree height (m)
1	Tropical forest tree	Ghana	RIEGL VZ-400	38.41
2	Tropical forest tree	Ghana	RIEGL VZ-400	34.18
3	Lowland tropical moist forest tree	Guyana	RIEGL VZ-400	34.19
4	Peat swamp forest tree	Indonesia	RIEGL VZ-400	26.47
5	Terra firme forest tree	Cameroon	Leica C10 Scanstation	38.73
6	Terra firme forest tree	Cameroon	Leica C10 Scanstation	22.45
7	Lodgepole pine	Canada	Optech Ilris HD	22.39
8	Norway spruce	Finland	Leica HDS6100	27.05
9	Sugar maple	Canada	Optech Ilris HD	23.25

undetected wood nodes in Fig. 9 are recovered successfully. As mentioned in Section 2.2, the nodes in the graph are the mode points, which are obtained by the Mean Shift segmentation in Section 2.1. Each mode point corresponds to one segment. Thus, the final wood points can be obtained by merging all the segments that corresponds to the wood nodes. The final wood points are shown in Fig. 10 (b).

3. Experimental results and analysis

To evaluate the performance of the proposed method, this paper adopted nine publicly available individual tree samples for the testing. The individual tree samples are provided by Moorthy et al. (2020), Xi et al. (2020) and Wang et al. (2020), respectively. Although there are many other tree samples in these three publicly available datasets, this paper only selected some representative tree points with different species and different structural features for the testing the robustness of the proposed method towards different forest environments. The validation data description for the tree samples are shown in Table 2. It can be found that there are seven different tree species that are concluded in these testing tree samples, including tropical forest tree, lowland tropical moist forest tree, peat swamp forest tree, terra firme forest tree, lodgepole pine, norway spruce and sugar maple. Thus, it will be useful for evaluating the stability and generalization of the proposed method towards different tree species. From Table 2, it can also be found that these nine tree samples are located in six different countries and are acquired using different laser scanners. Thus, it will be useful for testing the stability of the proposed method towards different forest environments and the points obtained by different laser scanners. As shown in Fig. 11, the nine tree samples show different tree structures and the tree heights are varying from 22.39 m to 38.73 m (Table 2). These characteristics also help to evaluate the generalization and uncertainty of the proposed method. All the nine individual trees are manually classified as wood and leaf using the visual software, such as CloudCompare. Thus, it will be easy to evaluate the performance of the proposed method.

In this paper, three kinds of accuracy indicators, including accuracy, F1 score and Kappa coefficient were calculated to access the performance of the proposed method. These three accuracy indicators can be calculated according to the confusion matrix as tabulated in Table 3. Accuracy represents the ratio of correctly classified points to the total number of point clouds. It can be calculated according to Eq. (11). The F1 score (F_1) can be calculated using precision (P) and recall (R) according to Eq. (14). Precision (P) represents the ratio of the classified true positive samples to the classified positive samples, which can be calculated using Eq. (12). Recall (R) represents the ratio of classified true positive samples to the reference positive samples, which can be calculated using Eq. (13). It should be noted that when the wood points are treated as a positive class, the F1 score for wood can be calculated. When the leaf points are treated as a positive class, the F1 score for leaf can be calculated. Thus, this paper calculates F1 scores for wood and leaf, respectively. Kappa coefficient is another indicator for accessing the classification accuracy, which can be calculated using proportionate agreement (po) and probability of random agreement (pe) according to Eqs. (15)–(17).

$$Accuracy = \frac{T_P + T_N}{T_P + F_P + F_N + T_N} \tag{11}$$

$$P = \frac{T_P}{T_P + F_P} \tag{12}$$

$$R = \frac{T_P}{T_P + F_N} \tag{13}$$

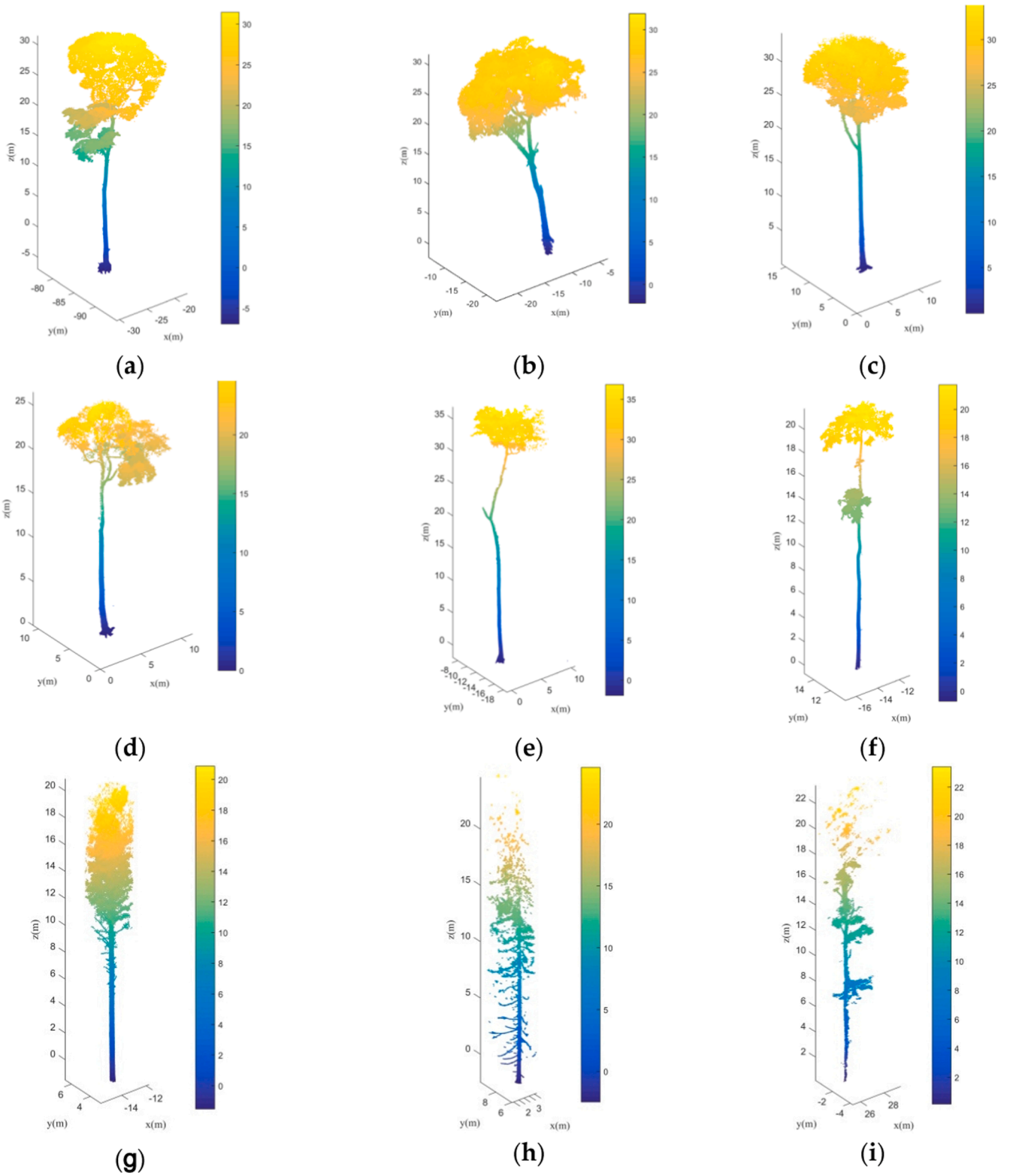

Fig. 11. The datasets used for testing. (**a**) and (**b**) are tropical forest trees located in Ghana; (c) is the lowland tropical moist forest tree located in Guyana; (d) is the peat swamp forest tree located in Indonesia; (e) and (f) are terra firme forest trees located in Cameroon; (g) is the lodgepole pine located in Canada; (h) is the Norway spruce located in Finland and (i) is the sugar maple located in Canada. (a) and (b) are the datasets provided by Moorthy et al. (2020); (c), (d), (g), (h) and (i) are the datasets provided by Xi et al. (2020); (e) and (f) are the datasets provided by Wang et al. (2020). The tree points are colored based on the elevation of each point.

$$F_1 = 2*\frac{P*R}{P+R} \tag{14}$$

$$po = (T_P + T_N)/N \tag{15}$$

$$pe = ((T_P + F_N)*(T_P + F_P) + (F_P + T_N)*(F_N + T_N))/(N*N) \tag{16}$$

$$kappa = (po - pe)/(1 - pe) \tag{17}$$

Table 3
Confusion matrix.

		Classification	
		Wood	Leaf
Reference	Wood	T_P	F_N
	Leaf	F_P	T_N

Table 4
The accuracy indicators calculation results of the proposed method.

Tree samples	Accuracy	F1 score wood	F1 score leaf	κappa
1	0.914	0.867	0.936	0.803
2	0.931	0.902	0.947	0.849
3	0.925	0.868	0.948	0.816
4	**0.970**	**0.981**	0.928	0.909
5	0.969	0.968	**0.970**	**0.938**
6	0.928	0.900	0.944	0.844
7	0.826	0.794	0.849	0.644
8	0.767	0.749	0.782	0.532
9	0.801	0.806	0.795	0.605
AVE	0.892	0.871	0.900	0.771

Table 5
The comparison of average of accuracy, F1 score for wood, F1 score for leaf and kappa coefficient.

	Accuracy	F1 score wood	F1 score leaf	κappa
LeWoS_NoRegu (Wang et al., 2020)	0.848	0.794	0.864	0.665
LeWoS_Regu (Wang et al., 2020)	0.890	0.845	0.903	0.753
CANUPO (Brodu and Lague, 2012)	0.820	0.794	0.821	0.629
The proposed method	0.892	0.871	0.900	0.771

where T_p is the number of the correctly classified wood points. F_N is the number of wood points that are wrongly classified as leaf points. F_P is the number of leaf points that are wrongly classified as wood points. T_N is the number of the correctly classified leaf points. P is the ratio of the classified true positive samples to the classified positive samples. R is the ratio of classified true positive samples to the reference positive samples. F_1 is the F1 score, which is a harmonic average of precision (P) and recall (R).N in Eqs. (16) and (17) is the number of all the points. po is the proportionate agreement, while pe is the probability of random agreement. $kappa$ is the Kappa coefficient, which measures the relationship between beyond-chance agreement and expected disagreement.

The four accuracy indicators (Accuracy, F1 score for wood, F1 score for leaf and kappa) calculation results of the proposed method are shown in Table 4. It can be found that in addition to sample8, all the accuracies of other eight tree samples are higher than 0.8. As a result, the average accuracy of these nine tree samples is 0.892. This indicates that the proposed method has a good wood and leaf classification performance towards different trees with different structural features. In terms of F1 score, both the average F1 scores for wood and leaf are higher than 0.85. Thus, it can be concluded that the proposed method has a good balance

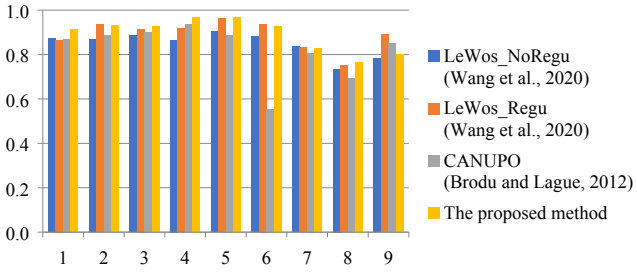

Fig. 12. The accuracy of the four classification results towards these nine tree samples.

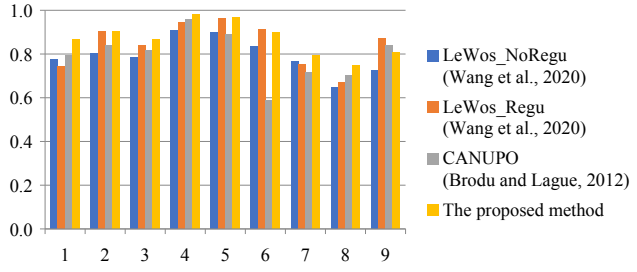

Fig. 13. The F1 score for wood of the four classification results towards these nine tree samples.

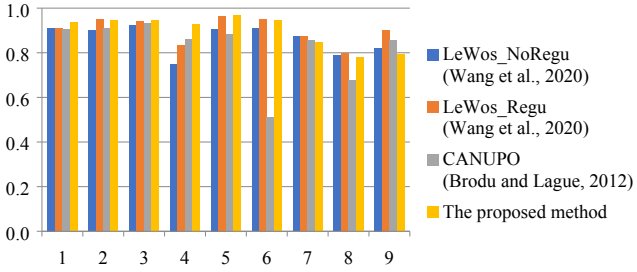

Fig. 14. The F1 score for leaf of the four classification results towards these nine tree samples.

Table 6
The comparison of Type I and Type II errors.

Tree samples	Type I error				Type II error			
	LeWoS_NoRegu (Wang et al., 2020)	LeWoS_Regu (Wang et al., 2020)	CANUPO (Brodu and Lague, 2012)	The proposed method	LeWoS_NoRegu (Wang et al., 2020)	LeWoS_Regu (Wang et al., 2020)	CANUPO (Brodu and Lague, 2012)	The proposed method
1	0.326	0.401	0.229	0.141	0.032	0.004	0.082	0.060
2	0.211	0.130	0.146	0.086	0.091	0.028	0.097	0.060
3	0.305	0.274	0.261	0.180	0.033	0.003	0.029	0.030
4	0.165	0.101	0.074	0.029	0.013	0.004	0.026	0.036
5	0.108	0.048	0.063	0.047	0.085	0.027	0.160	0.015
6	0.170	0.097	0.110	0.100	0.089	0.044	0.637	0.056
7	0.349	0.390	0.423	0.194	0.032	0.009	0.028	0.159
8	0.504	0.479	0.256	0.291	0.033	0.030	0.360	0.178
9	0.385	0.199	0.146	0.109	0.071	0.035	0.157	0.278
AVE	0.280	0.235	0.190	0.131	0.053	0.020	0.175	0.097

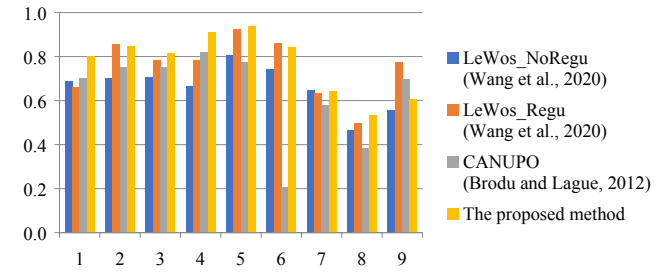

Fig. 15. The kappa coefficient of the four classification results towards these nine tree samples.

when classifying wood and leaf. In other words, the proposed method does not tend to classify more wood points as leaf points. Meanwhile, the method also does not tend to classify more leaf points as wood points. Although the kappa coefficient is not as good as the accuracy, the average of kappa coefficient is still higher than 0.75. Thus, it can be concluded that the proposed method has a good generation towards different tree species.

To objectively evaluate the proposed method, two other famous wood and leaf classification methods, namely LeWoS and CANUPO are also adopted for testing their performance towards these six tree samples. LeWoS was proposed by Wang et al. (2020) recently. LeWoS belongs to the geometric feature based methods. Different from the other point-wise approaches, LeWoS first segments the tree points into clusters using a graph-based segmentation method. By calculating the linearity and size of each segment, the tree points can be classified as wood and leaf points, respectively. To obtain an improved labeling result, Wang et al. (2020) applied the class regularization technique to the classification result mentioned above. Thus, LeWoS can provide two wood and leaf classification results based on with or without regularization. In LeWoS, there is only one parameter that needs to be determined. The parameter is the threshold for controlling the feature similarity. Wang et al. (2020) set the threshold to 0.15 in their study. Thus, in this paper we also adopted this default value for testing the performance of the LeWoS. CANUPO was proposed by Brodu and Lague (2012). CANUPO is a classic machine learning method for point clouds classification since it calculates multiscale geometric features for each point. In so doing, more geometric difference between wood and leaf points can be captured. Thus, the classification result will be better. Moreover, calculating multiscale geometric features will avoid selecting the optimal neighboring size when calculating the single-scale feature. Therefore, CANUPO is a representative supervised learning method. In CANUPO, only two parameters need to be set. One is the scales, while

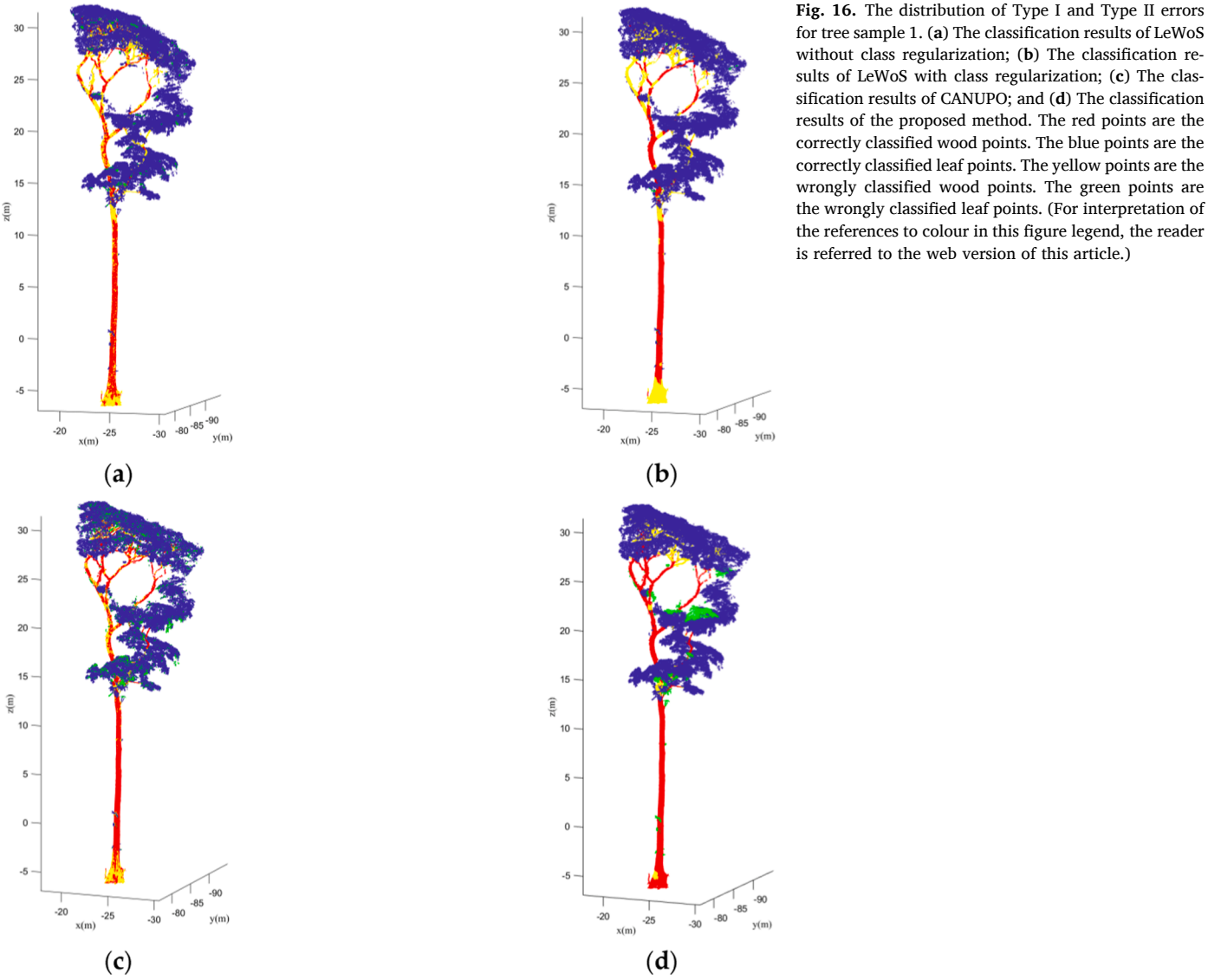

Fig. 16. The distribution of Type I and Type II errors for tree sample 1. (**a**) The classification results of LeWoS without class regularization; (**b**) The classification results of LeWoS with class regularization; (**c**) The classification results of CANUPO; and (**d**) The classification results of the proposed method. The red points are the correctly classified wood points. The blue points are the correctly classified leaf points. The yellow points are the wrongly classified wood points. The green points are the wrongly classified leaf points. (For interpretation of the references to colour in this figure legend, the reader is referred to the web version of this article.)

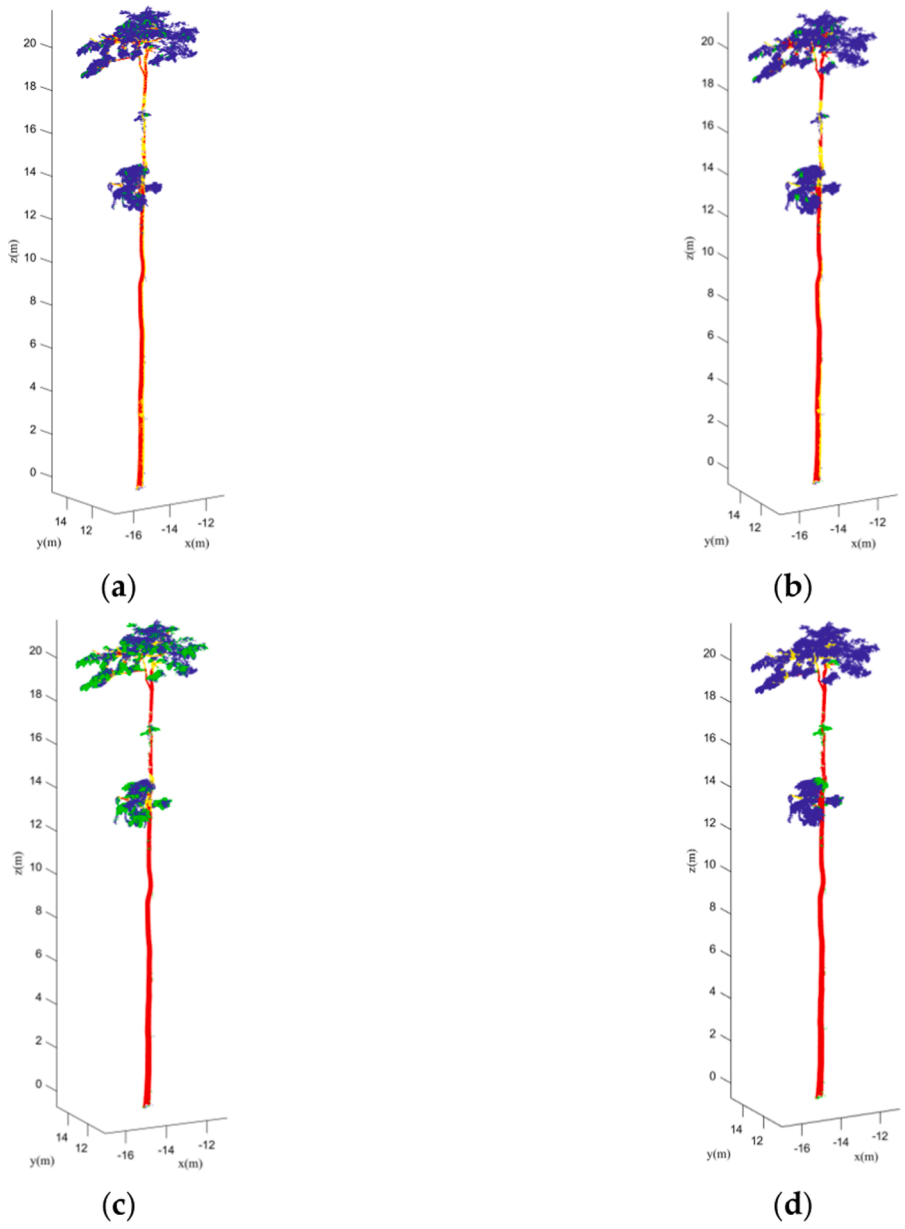

Fig. 17. The distribution of Type I and Type II errors for tree sample 6. (**a**) The classification results of LeWoS without class regularization; (**b**) The classification results of LeWoS with class regularization; (**c**) The classification results of CANUPO; and (**d**) The classification results of the proposed method. The red points are the correctly classified wood points. The blue points are the correctly classified leaf points. The yellow points are the wrongly classified wood points. The green points are the wrongly classified leaf points. (For interpretation of the references to colour in this figure legend, the reader is referred to the web version of this article.)

the other one is the number of maximum core points. The scales determine the geometric features calculated in different neighboring sizes. Brodu and Lagure (2012) set the default number of scales as 10. The minimum scale is 0.1 m, while the maximum scale is 1 m. The core points are the sub-sampling points of the scene, which can speed up the efficiency of the multi-scale features calculation. Brodu and Lagure (2012) set the default number of core points as 10000. In this paper, we applied all these default parameters in CANUPO to realize the wood and leaf separation. The reason for selecting LeWoS and CANUPO for comparison is that LeWoS is an open-source Matlab tool and CANUPO has been integrated in a famous free software named CloudCompare. Thus, the comparison results using these two methods will be objective.

This paper calculated the average value of the four accuracy indicators (Accuracy, F1 score for wood, F1 score for leaf and kappa) as tabulated in Table 5. It is easy to find that the proposed method performs the best in terms of accuracy, F1 score for wood and kappa. The average F1 score for leaf of the proposed method is only slightly lower than that of the LeWoS with regularization. The average accuracy of the proposed method is nearly 0.9. It indicates that although seven different tree species were testing in this paper, most tree points are correctly classified as wood and leaf, respectively. Thus, it can be concluded that the proposed method has a good wood and leaf classification performance towards different tree samples with different tree species. The generalization of the proposed method is good. Meanwhile, as shown in Table 2, the tree samples were acquired using different laser scanners from six different countries. Both the average F1 scores for wood and leaf of the proposed method are higher than 0.85. It means that the proposed method has a good balance when detecting woods and leaves from different forest environments. Therefore, the stability of the proposed method is better when comparing with other two methods.

To further analysis the classification errors, this paper further calculated Type I and Type II errors of these four classification results. Type I error is also named as omission error. When wood is treated as a positive class, Type I error means the percentage of wood points misclassified as leaf points. Type II error is also named as commission error. That is the percentage of leaf points misclassified as wood points. According to the confusion matrix tabulated in Table 3, Type I and Type II errors can be calculated as Eqs. (18) and (19).

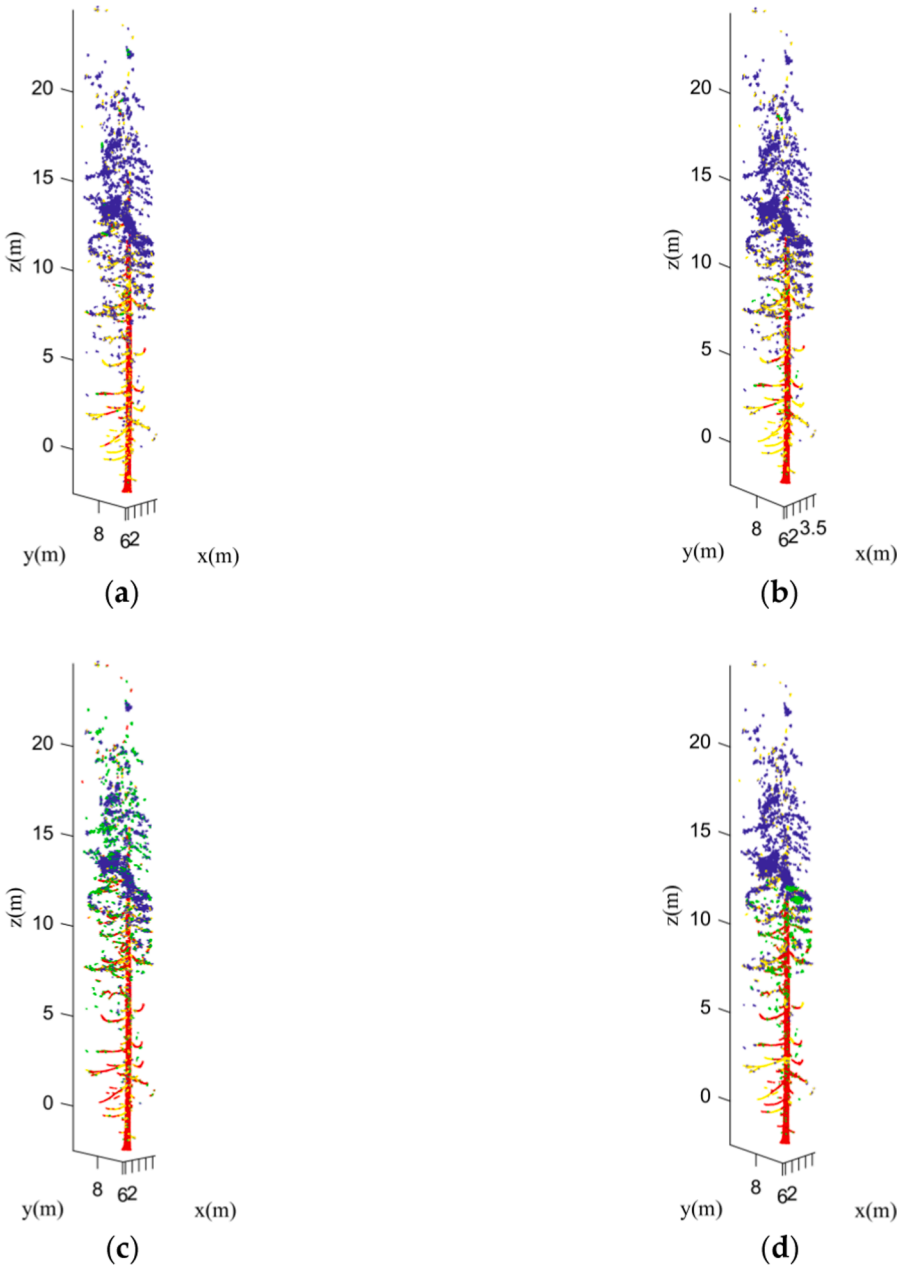

Fig. 18. The distribution of Type I and Type II errors for tree sample 8. (**a**) The classification results of LeWoS without class regularization; (**b**) The classification results of LeWoS with class regularization; (**c**) The classification results of CANUPO; and (**d**) The classification results of the proposed method. The red points are the correctly classified wood points. The blue points are the correctly classified leaf points. The yellow points are the wrongly classified wood points. The green points are the wrongly classified leaf points. (For interpretation of the references to colour in this figure legend, the reader is referred to the web version of this article.)

Table 7
Parameter settings in this paper.

Tree samples	Bandwidth h	Radius r	FrequencyRatio δ	Verticality threshold η
1	0.5	2.0	0.5	0.125
2	0.65	2.0	0.5	0.125
3	0.5	2.0	0.5	0.125
4	0.3	1.5	0.5	0.125
5	0.3	1.5	0.5	0.125
6	0.3	1.5	0.5	0.125
7	0.3	1.5	0.5	0.125
8	0.3	1.5	0.5	0.125
9	0.3	1.5	0.5	0.125

$$T_1 = \frac{F_N}{T_P + F_N} \tag{18}$$

$$T_2 = \frac{F_P}{F_P + T_N} \tag{19}$$

Type I and Type II errors of these four classification results are shown in Table 6. It is easy to find that the proposed method achieved the smallest average Type I error (0.131). It indicates that the proposed method can detect as more wood points as possible. Although Type II error of the proposed method is a little larger than that of the LeWoS with regularization, Type I error of the proposed method is much lower than that of the LeWoS with regularization. Moreover, the proposed method can achieve a good balance between Type I and Type II errors. In the proposed method, both the average of Type I and Type II errors are smaller than 0.15. Comparing with other methods, Type I error of the LeWoS without regularization is over five times of its Type II error, while Type I error of the LeWoS with regularization is over ten times of its Type II error.

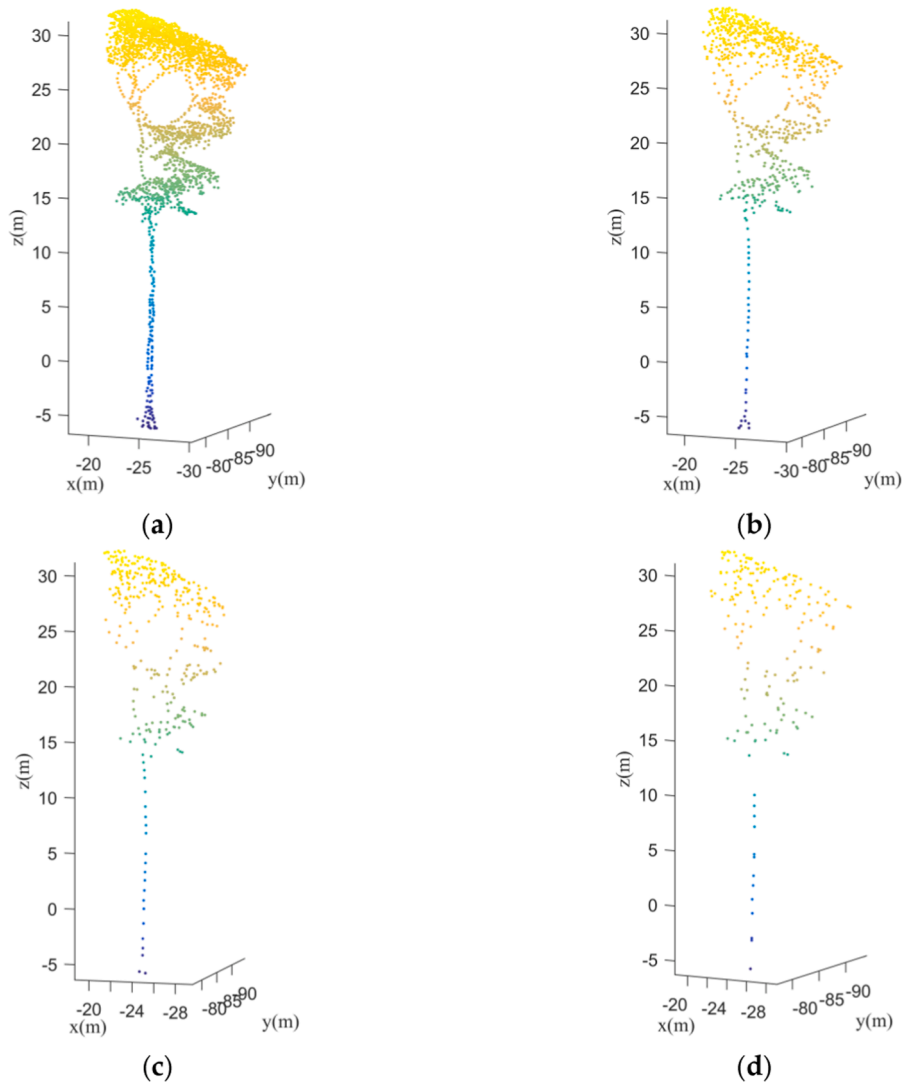

Fig. 19. The mode points acquisition results using different bandwidths. (**a**) Bandwidth is 0.3; (**b**) Bandwidth is 0.5; (**c**) Bandwidth is 0.7; (**d**) Bandwidth is 0.9.

4. Discussion

For accurate comparative analysis, four indicators (Accuracy, F1 score for wood, F1 score for leaf and kappa) of the four classification results (LeWoS_NoRegu, LeWoS_Regu, CANUPO and the proposed method) are shown in Figs. 12–15. Here, LeWoS_NoRegu is the LeWoS classification result without regularization, while LeWoS_Regu is the LeWoS classification result with regularization.

Fig. 12 shows the accuracy comparison results. It can be found that the proposed method achieved five highest accuracies in the nine tree samples. In addition to the tree sample 8, the proposed methods can achieve accuracies higher than 0.8 for all the other eight samples. As shown in Table 2, seven different tree species are concluded in the nine tree samples. Thus, it can be concluded that the proposed method has a good generalization towards different tree species. In terms of sample 8, all the accuracies of the four classification results are lower than 0.8. From 11 (h), it can be found that this Norway spruce has many tiny branches along the tree stem. These tiny branches are easily misclassified as leaves. This can also be found from the error distributions in Fig. 18. Although the classification accuracy of sample 8 is low, the proposed method still performs the best when comparing with other three classification results. Moreover, it can be found that after class regularization, LeWoS can achieve a better classification result than that of the LeWoS without regularization. Figs. 13 and 14 are the comparison results of F1 scores for wood and leaf. In terms of F1 score for wood, the proposed method achieved six highest F1 scores in the nine tree samples. As a result, the average F1 score for wood of the proposed method is much higher than that of other three classification results (Table 5). In addition to sample 8, the three methods performed worse towards sample 7. It can be found from Fig. 13, the F1 scores for wood of the four classification results towards sample 7 are lower than 0.8. From Fig. 11 (g), it can be found that sample 7 is the lodgepole pine. Generally, the branches or the stem for the pine are difficult for detecting since there is lots of occlusion by the leaves. Meanwhile, some dense leaves are prone to be misclassified as woods. In terms of the F1 score for leaf, all the three methods perform well. As a result, the average F1 scores for leaf of the four classification results are higher than 0.8 (Table 5). In terms of the kappa coefficient, all the methods perform worse towards sample 8. The kappa coefficients for the four classification results are all smaller than 0.6. Thus, how to detect the tiny branches for the Norway spruce is still challenging.

For visual analysis of these two kinds of errors, this paper selected three tree samples (1, 6 and 8) to show their error distributions. Tree sample 1 is selected because all the three methods tend to achieve larger Type I error towards this sample. Tree sample 6 is selected because CANUPO obtains a very poor classification results in terms of Type II error. Tree sample 8 is selected because all the three methods perform worse towards this sample no matter accuracy or kappa coefficient is

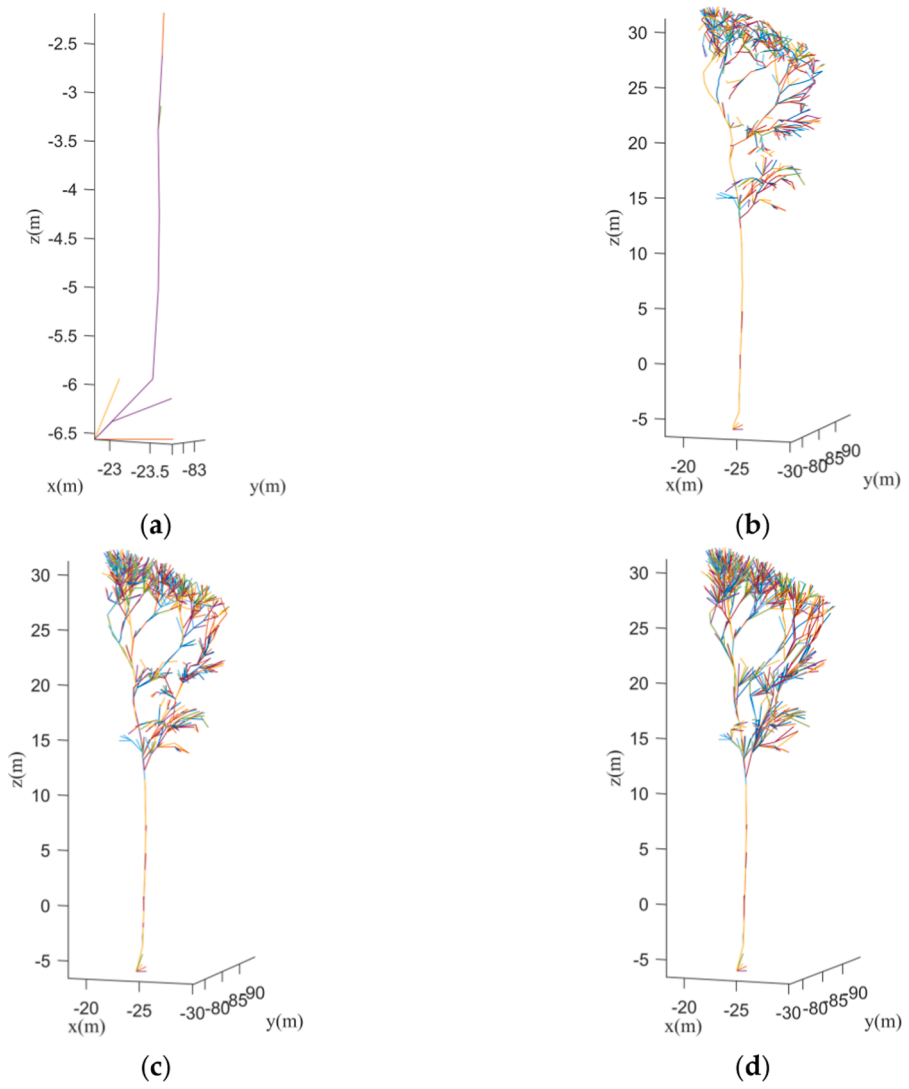

Fig. 20. The paths of each node to the base node in the graph built using different neighboring radiuses. (**a**) Radius is 1.0 m; (**b**) Radius is 1.5 m; (**c**) Radius is 2.0 m; and (**d**) Radius is 2.5 m.

adopted. The distributions of Type I and Type II errors are shown in Figs. 16–18. In these figures, the red points are the correctly classified wood points. The blue points are the correctly classified leaf points. The yellow points are the wrongly classified wood points. The green points are the wrongly classified leaf points. From Fig. 16 (d), it is easy to find that the proposed method achieved a good classification result. More wood points are correctly classified. Especially for branches, the proposed method performs much better than the other three classification results (Fig. 16 (a-c)). Moreover, it can also be found that the misclassified points of LeWoS and CANUPO are dispersed distribution, while the misclassified points of the proposed method mainly concentrated in the canopy area. The error spatial distribution has a great influence on the following forest applications, such as tree models building. The dispersed misclassified points will influence the modeling accuracy greatly. From Fig. 17 (a) and (b), it can be found that some trunk points are misclassified as leaf points by LeWoS. Although using class regularization the class labeling results will be smoothed, some tree wood points can also be filtered in this regularization process as shown in Fig. 17 (b). As tabulated in Table 6, CANUPO achieved a very large Type II error (0.637) for tree sample 6. From Fig. 17 (c), it can be found that many leaf points are misclassified as wood points. It may be because the geometric features of these leaf points are similar to the ones of wood points in this tree sample. These are also the drawbacks of point-wise supervised learning method based on geometric features. Satisfactory classification results are not always obtained in all cases. Compared to other three classification results, the proposed method achieved a much better wood and leaf classification result as shown in Fig. 17 (d). Fig. 18 shows the error distributions of the four classification results in terms of sample 8. As shown in Table 6, all the three methods obtained larger Type I or Type II errors for sample 8. This can also be found in Fig. 18 (a-d). Compared with the results of the LeWoS method (Fig. 18 (a) and (b)), CANUPO and the proposed method can detect more tiny branches (Fig. 18 (c) and (d)). However, there are many misclassified points that are dispersed distribution in the CANUPO classification result. Thus, it can be found that although all the three methods have difficulties in the wood-leaf separating towards the Norway spruce, the proposed method can still achieve a better classification result.

Four main parameters are involved in this paper, namely bandwidth h in Eq. (1), radius r in Eq. (2), frequency ratio δ in Eq. (7) and verticality threshold η in Eq. (8). The parameter settings for the nine tree samples in this paper are tabulated in Table 7. It can be found that both δ and η are set as fixed constant values in this study. To show the influence of these parameters, this paper selected tree sample 1 for the testing.

The bandwidth h mainly affects the Mean Shift segmentation results. Since each segment corresponds to a mode point, the bandwidth h has an influence on the mode points acquisition. Fig. 19 (a-d) is mode points

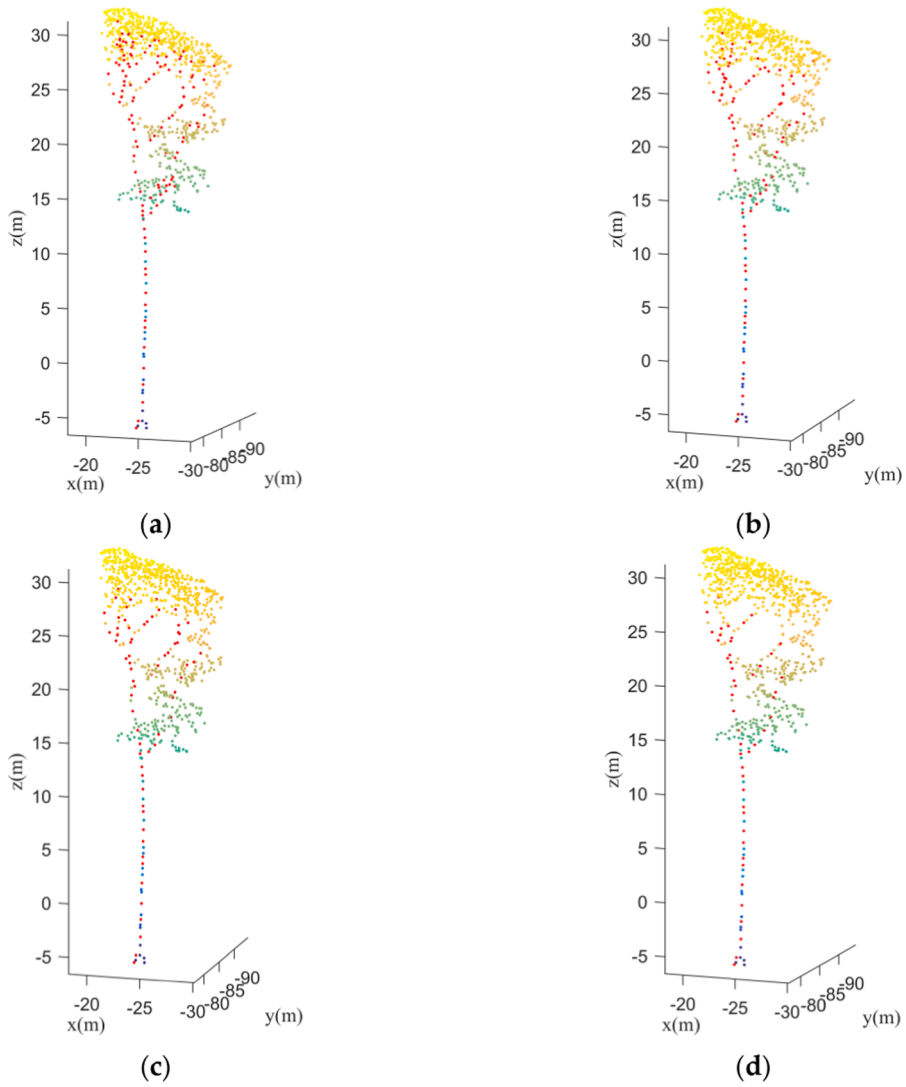

Fig. 21. Wood nodes detection using different frequency ratios. (**a**) Ratio is 0.3; (**b**) Ratio is 0.4; (**c**) Ratio is 0.5; and (**d**) Ratio is 0.6. The red points are the detected wood nodes. (For interpretation of the references to colour in this figure legend, the reader is referred to the web version of this article.)

acquisition results using four different bandwidths (0.3, 0.5, 0.7 and 0.9). It is easy to find that when the bandwidth h is smaller, more mode points can be acquired as shown in Fig. 19 (a). However, more mode points will lead to a complicated network graph. When the bandwidth h is larger, less mode points can be acquired. However, less mode points cannot reflect the tree structure as shown in Fig. 19 (d). It will be difficult for the following mode points evolution. It is really true that when h is larger, some leaf points and wood points may be segmented as one segment. However, even though the bandwidth h is set smaller, the misclassification is still possible. Although when h is smaller the possibility of wood-leaf points misclassified together will be lower, the classification results will be over-segmentation. Especially, the stem will be segmented into many pieces. Thus, the segmentation results cannot be more precise. Meanwhile, the over-segmentation means more mode points can be acquired. More mode points don't only mean more complex graph, but the stem points cannot be detected completely and accurately. As shown in Fig. 19 (a), there are many mode points in the stem. When the shortest path analysis is conducted to this corresponding graph, only parts of stem nodes can be detected as wood nodes. It is because that not all the stem nodes own a higher visiting frequency. Thus, the omission error for wood detection will be larger. This finding can also be found in the literature concluded by Vicari et al. (2019).

In general, the bandwidth should be slightly larger than the trunk diameter. In so doing, the trunk points will be replaced as mode points in a line. Meanwhile, the mode points can still reflect the tree structure as shown in Fig. 19 (b).

The neighboring radius r mentioned in Eq. (2) mainly affects the structure of the built graph. Obviously, a larger radius means more neighboring points will form edges, while a smaller radius means less neighboring points will form edges. Fig. 20 shows the paths of each node to the base node in the graph built using different neighboring radiuses. In Fig. 20 (a), it can be found that only some short paths are obtained. It is because the neighboring radius is set too small, many nodes in the graph cannot have a direct path to the base node. Obviously, this graph cannot be used for the following wood nodes extraction. When the neighboring radius is set larger, more edges will be involved in the graph and the built graph will be complicated. As shown in Fig. 20 (b-d), the paths of each node to the base node turn detailed and abundant. However, larger radius means more complex graph, what followed is the process of generating the graph will be time consuming. In general, the radius setting should be according to the bandwidth. As mentioned above, a larger bandwidth will lead to less mode points. Thus, the distance between two neighboring mode points will be larger. To make the network graph connected, the neighboring radius should be larger. Moreover, to make the graph less complicated and improve implementation efficiency, the radius cannot be set too large. In this study, $r \in$

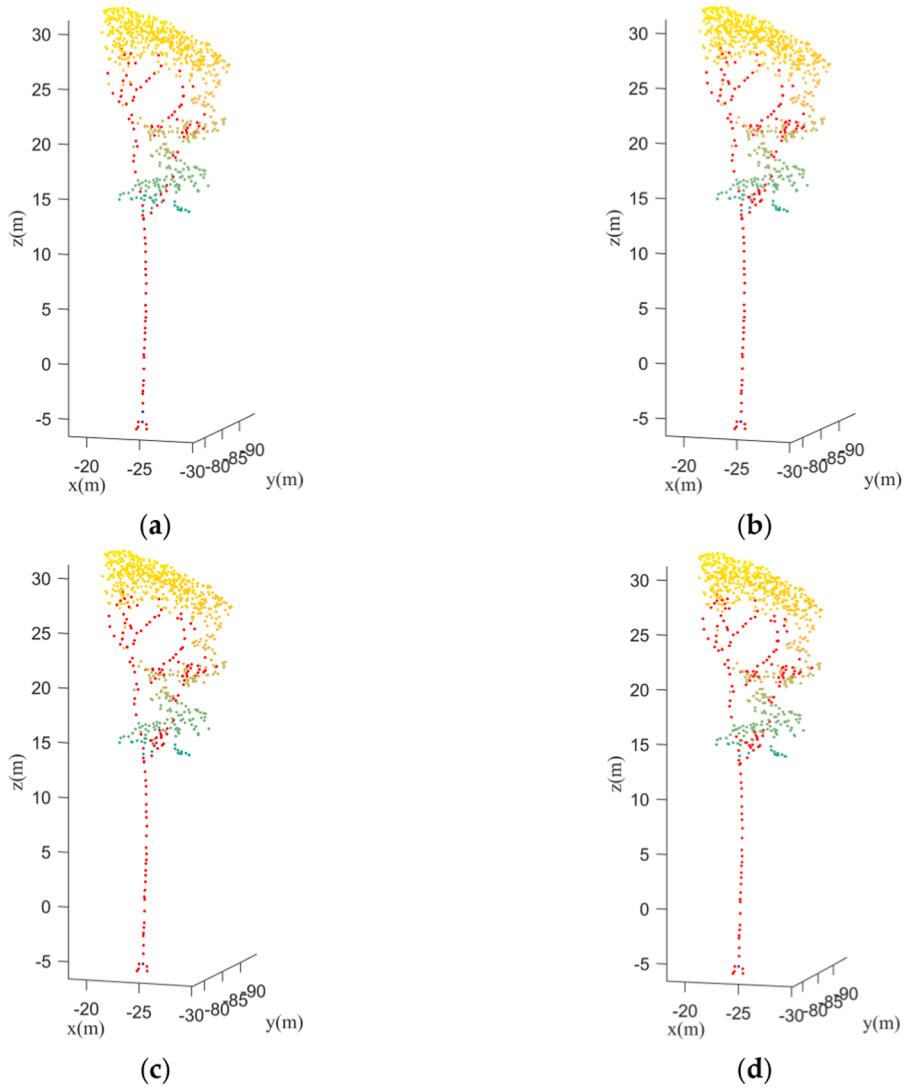

Fig. 22. Wood node evolution results based on different verticality thresholds. (**a**) Verticality threshold is 0.05; (**b**) Verticality threshold is 0.10; (**c**) Verticality threshold is 0.15; and (**d**) Verticality threshold is 0.20. The red points are the wood nodes after evolution. (For interpretation of the references to colour in this figure legend, the reader is referred to the web version of this article.)

$[1.5, 2.0]$ is appropriate for the tree samples.

The frequency ratio δ mentioned in Eq. (7) mainly affects how many nodes can be detected as wood nodes. Fig. 21 shows the wood detection results using different frequency ratios (0.3, 0.4, 0.5 and 0.6). It is easy to find that the smaller the ratio is the more wood nodes can be detected. That makes sense because when the ratio is set smaller, it means more nodes with lower visiting frequency will be detected as wood nodes. This can be found in Fig. 21 (a) and (b). Some leaf nodes in the canopy are misclassified as wood nodes. Conversely, when the ratio is larger the wood nodes on the branches cannot be detected successfully. It is because the visiting frequency of the leaf nodes on the branch is not as high as the nodes on the trunk. Thus, some wood nodes cannot be detected successfully when the ratio is set larger. In this study, the frequency ratio is set to 0.5 for all the tree samples.

The verticality threshold η is a key parameter for wood nodes evolution. The verticality threshold is adopted for evolving the nodes with similar verticality as wood nodes. Obviously, when the verticality threshold is small the evolved wood nodes will be less. As shown in Fig. 22 (a), some nodes on the branch cannot be evolved as wood nodes successfully. When the verticality threshold is large the evolved wood nodes will be more. As shown in Fig. 22 (d), some leaf nodes are misclassified as wood nodes after the evolution. In this study, when the verticality threshold is set between 0.1 and 0.15, the wood nodes can be evolved successfully while avoiding the leaf nodes wrongly evolved as wood nodes. In this paper, the verticality threshold is set to a constant value as 0.125.

In this study, seven kinds and nine tree samples were adopted for testing the performance of the proposed method and satisfied wood and leaf separation results were obtained. It must be admitted that we cannot test all the tree species for validating the robustness of the proposed method. Thus, several different representative tree species with distinguishable tree structures will be useful for testing the stability of the proposed method towards different forest environments. From Fig. 11, it can be found that all the nine tested tree samples are taller than 20 m. To evaluate the performance of the proposed method towards small trees, three low tree samples with different tree species are utilized for further testing. As shown in Fig. 23, (a), (c) and (e) are tree samples of Gliricidia sepium, Swietenia macrophylla and beech Buche. It can be found that all these three tree samples are lower than 10 m. Moreover, all these three tree samples are with distinguishable structures. Thus, these three tree samples will be representative for showing the robustness of the proposed method. In Fig. 23, (b), (d) and (f) are wood and leaf separation results of the Gliricidia sepium, Swietenia macrophylla and beech Buche. It can be found that the proposed method can achieve promising

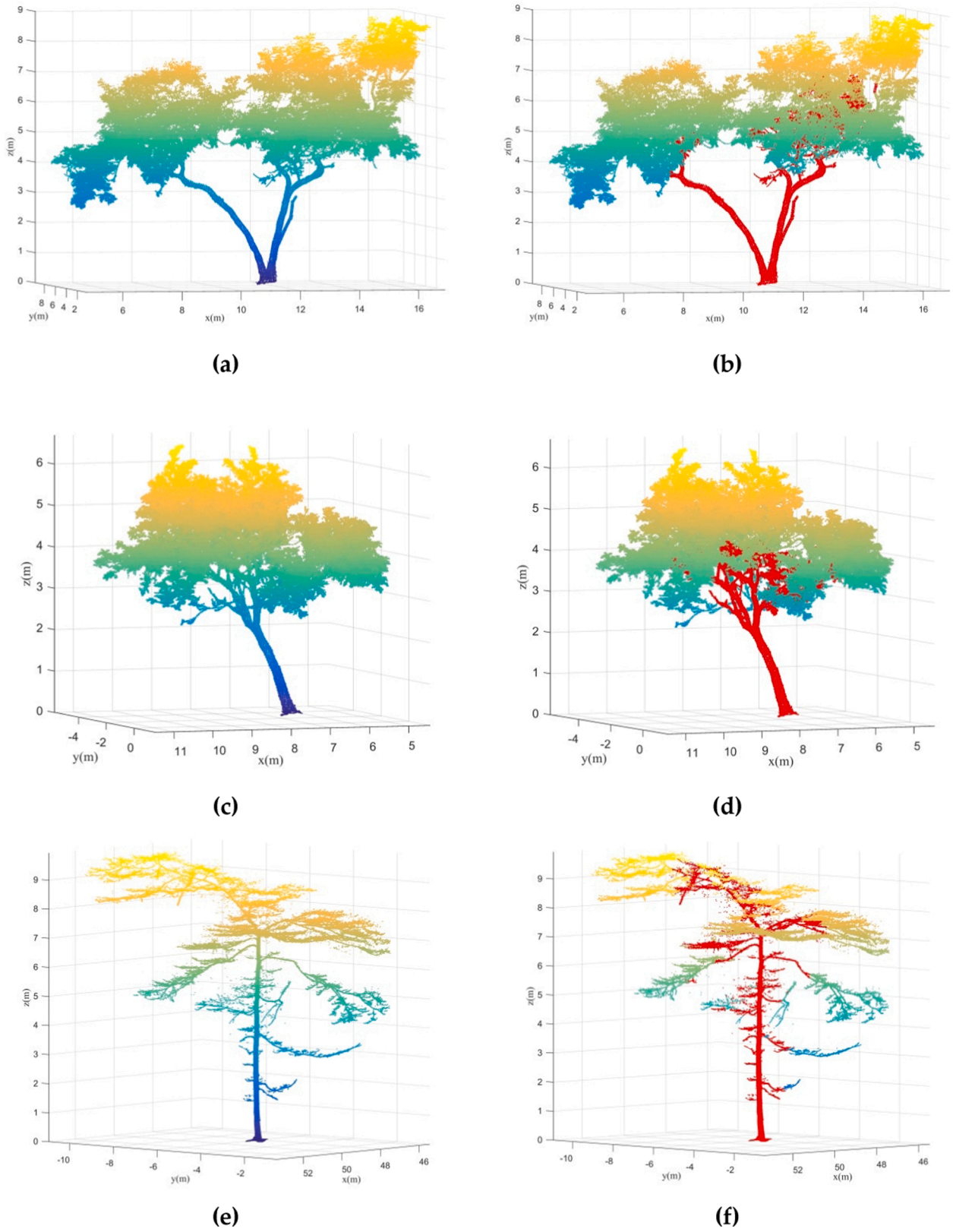

Fig. 23. Small tree samples and their corresponding wood and leaf separation results. **(a)**, **(c)** and **(e)** are tree samples of Gliricidia sepium, Swietenia macrophylla and beech Buche; **(b), (d)** and **(f)** are these tree samples' corresponding wood and leaf separation results.

classification results towards these three low tree samples. Although the three tree samples are with different tree species and different tree structures, the proposed method can detect stems and branches correctly for each tree sample. As a result, the classification accuracies for these three tree samples are all higher than 0.9. Thus, we can conclude that the proposed method can also obtain good wood and leaf classification results towards small trees.

5. Conclusion

Wood and leaf separation is a critical process for the forest post-applications. To classify wood and leaf points correctly from terrestrial LiDAR point clouds for the individual tree, this paper proposed a wood and leaf separation method based on mode points evolution. In the proposed method, the mode points are acquired using the Mean Shift method. Then all the mode points are used to construct a graph network. In so doing, the constructed graph will be less complicated and the point-wise classification will be transformed into the segment-wise classification. According to the path retracing result and nodes visiting frequency, the wood seed nodes can be detected. By setting three evolution constraints, all wood nodes can be evolved successfully. Finally, all the segments corresponding to these wood nodes are merged together to obtain the final classified wood points. Nine tree samples with different tree species are adopted for testing the performance of the proposed method. Experimental results show that the proposed method can achieve very good wood and leaf classification results. The average classification accuracy is 0.892. The average F1 score for wood is 0.871, while the average F1 score for leaf is 0.900. Compared with other two methods, namely LeWoS and CANUPO, the proposed method performs better. This paper also compared the Type I and Type II errors of these three methods. The proposed method can achieve the smallest average Type I error. Meanwhile, the proposed method can keep a good balance between the Type I and Type II errors. It means that the proposed method can detect the wood points effectively while removing the leaf points successfully. Although four parameters are involved in this study, frequency ratio and verticality threshold can be set constant values. Thus, the proposed method is easy to implement while owing the good wood and leaf classification performance.

Declaration of Competing Interest

The authors declare that they have no known competing financial interests or personal relationships that could have appeared to influence the work reported in this paper.

Acknowledgement

This research project was partly funded by the National Natural Science Foundation of China (NSF) (41801325, 41861052, 41874001), the Natural Science Foundation of Jiangxi Province (20192BAB217010), the China Post-Doctoral Science Foundation (2019M661858), Education Department of Jiangxi Province (GJJ170449), Key Laboratory for Digital Land and Resources of Jiangxi Province, East China University of Technology (DLLJ201806) and East China University of Technology Ph. D. Project (DHBK2017155).

Authors would like to thank Moorthy et al. (2020), Xi et al. (2020) and Wang et al. (2020) for providing the tested datasets located in different forest environments.

References

Beland, M., Widlowski, J., Fournier, R.A., Cote, J., Verstraete, M.M., 2011. Estimating leaf area distribution in savanna trees from terrestrial lidar measurements. Agr. Forest Meteorol. 151, 1252–1266.

Brodu, N., Lague, D., 2012. 3D terrestrial lidar data classification of complex natural scenes using a multi-scale dimensionality criterion: Applications in geomorphology. ISPRS J. Photogramm. 68, 121–134.

Calders, K., Newnham, G., Burt, A., Murphy, S., Raumonen, P., Herold, M., Culvenor, D., Avitabile, V., Disney, M., Armston, J., 2015. Nondestructive estimates of above-ground biomass using terrestrial laser scanning. Methods Ecol. Evol. 6, 198–208.

Cheng, Y.Z., 1995. Mean shift, mode seeking, and clustering. IEEE T. Pattern Anal. 17, 790–799.

Cote, J., Fournier, R.A., Egli, R., 2011. An architectural model of trees to estimate forest structural attributes using terrestrial lidar. Environ. Modell. Softw. 26, 761–777.

Dai, W., Yang, B., Dong, Z., Shaker, A., 2018. A new method for 3D individual tree extraction using multispectral airborne LiDAR point clouds. ISPRS J. Photogramm. 144, 400–411.

Danson, F.M., Gaulton, R., Armitage, R.P., Disney, M., Gunawan, O., Lewis, P., Pearson, G., Ramirez, A.F., 2014. Developing a dual-wavelength full-waveform terrestrial laser scanner to characterize forest canopy structure. Agr. Forest Meteorol. 198, 7–14.

Danson, F.M., Sasse, F., Schofield, L.A., 2018. Spectral and spatial information from a novel dual-wavelength full-waveform terrestrial laser scanner for forest ecology. Interface Focus 8.

Dong, T., Zhang, X., Ding, Z., Fan, J., 2020. Multi-layered tree crown extraction from lidar data using graph-based segmentation. Comput. Electron. Agr. 170.

Fang, W., Huang, X., Zhang, F., Li, D., 2015. Intensity correction of terrestrial laser scanning data by estimating laser transmission function. IEEE T. Geosci. Remote. 53, 942–951.

Ferrara, R., Virdis, S.G.P., Ventura, A., Ghisu, T., Duce, P., Pellizzaro, G., 2018. An automated approach for wood-leaf separation from terrestrial lidar point clouds using the density based clustering algorithm DBSCAN. Agr. Forest Meteorol. 262, 434–444.

Hackenberg, J., Wassenberg, M., Spiecker, H., Sun, D., 2015. Non destructive method for biomass prediction combining TLS derived tree volume and wood density. Forests 6, 1274–1300.

Henning, J.G., Radtke, P.J., 2006. Detailed stem measurements of standing trees from ground-based scanning lidar. Forest Sci. 52, 67–80.

Hu, X., Wei, C., Xu, W., 2017. Adaptive mean shift-based identification of individual trees using airborne LiDAR data. Remote Sens.-Basel. 9, 148.

Kankare, V., Holopainen, M., Vastaranta, M., Puttonen, E., Yu, X., Hyyppa, J., Vaaja, M., Hyyppa, H., Alho, P., 2013. Individual tree biomass estimation using terrestrial laser scanning. ISPRS J. Photogramm. 75, 64–75.

Li, S., Dai, L., Wang, H., Wang, Y., He, Z., Lin, S., 2017. Estimating leaf area density of individual trees using the point cloud segmentation of terrestrial lidar data and a voxel-based model. Remote Sens.-Basel. 9.

Li, Z., Douglas, E., Strahler, A., Schaaf, C., Yang, X.Y., Wang, Z.S., Yao, T., Zhao, F., Saenz, E.J., Paynter, I., 2013. Separating leaves from trunks and branches with dual-wavelength terrestrial lidar scanning. IEEE International Symposium on Geoscience and Remote Sensing IGARSS 3383–3386.

Liang, X., Hyyppa, J., Kaartinen, H., Lehtomaki, M., Pyorala, J., Pfeifer, N., Holopainen, M., Brolly, G., Pirotti, F., Hackenberg, J., 2018. International benchmarking of terrestrial laser scanning approaches for forest inventories. ISPRS J. Photogramm. 144, 137–179.

Lin, Y., Herold, M., 2016. Tree species classification based on explicit tree structure feature parameters derived from static terrestrial laser scanning data. Agr. Forest Meteorol. 216, 105–114.

Livny, Y., Yan, F., Olson, M., Chen, B., Zhang, H., El-Sana, J., 2010. Automatic reconstruction of tree skeletal structures from point clouds. Acm T, Graphic, p. 29.

Ma, L., Zheng, G., Eitel, J.U.H., Moskal, L.M., He, W., Huang, H., 2016. Improved salient feature-based approach for automatically separating photosynthetic and nonphotosynthetic components within terrestrial lidar point cloud data of forest canopies. IEEE T. Geosci. Remote. 54, 679–696.

Moorthy, S.M.K., Calders, K., Vicari, M.B., Verbeeck, H., 2020. Improved supervised learning-based approach for leaf and wood classification from lidar point clouds of forests. Ieee T. Geosci. Remote. 58, 3057–3070.

Olofsson, K., Holmgren, J., Olsson, H., 2014. Tree stem and height measurements using terrestrial laser scanning and the RANSAC algorithm. Remote Sens.-Basel. 6, 4323–4344.

Penasa, L., Franceschi, M., Preto, N., Teza, G., Polito, V., 2014. Integration of intensity textures and local geometry descriptors from terrestrial laser scanning to map chert in outcrops. ISPRS J. Photogramm. 93, 88–97.

Strimbu, V.F., Strimbu, B.M., 2015. A graph-based segmentation algorithm for tree crown extraction using airborne lidar data. ISPRS J. Photogramm. 104, 30–43.

Tan, K., Cheng, X., 2015. Intensity data correction based on incidence angle and distance for terrestrial laser scanner. J. Appl. Remote Sens. 9.

Tan, K., Cheng, X., 2016. Correction of incidence angle and distance effects on TLS intensity data based on reference targets. Remote Sens.-Basel. 8.

Tan, K., Zhang, W., Dong, Z., Cheng, X., Cheng, X., 2021. Leaf and wood separation for individual trees using the intensity and density data of terrestrial laser scanners. IEEE T. Geosci. Remote 1–13.

Tao, S., Guo, Q., Xu, S., Su, Y., Li, Y., Wu, F., 2015. A geometric method for wood-leaf separation using terrestrial and simulated lidar data. Photogramm. Eng. Rem. S. 81, 767–776.

Vicari, M.B., Disney, M., Wilkes, P., Burt, A., Calders, K., Woodgate, W., 2019. Leaf and wood classification framework for terrestrial lidar point clouds. Methods Ecol. Evol. 10, 680–694.

Vosselman, G., Maas, H.G., 2010. Airborne and terrestrial laser scanning. DBLP.

Wan, P., Zhang, W., Jin, S., Wang, T., Yang, S., Yan, G., 2020. Plot-level wood-leaf separation of trees using terrestrial lidar data based on segmentwise geometric feature classification method. Remote Sens.-Basel. in press.

Wang, D., Hollaus, M., Pfeifer, N., 2017. Feasibility of machine learning methods for separating wood and leaf points from terrestrial laser scanning data. ISPRS Ann. Photogramm., Remote Sens. Spatial Informati. Sci. 157–164.
Wang, D., Takoudjou, S.M., Casella, E., 2020. LeWoS: A universal leaf-wood classification method to facilitate the 3D modelling of large tropical trees using terrestrial lidar. Methods Ecol. Evol. 11, 376–389.
Wang, Y., Pyorala, J., Liang, X., Lehtomaki, M., Kukko, A., Yu, X., Kaartinen, H., Hyyppa, J., 2019. In situ biomass estimation at tree and plot levels: What did data record and what did algorithms derive from terrestrial and aerial point clouds in boreal forest. Remote Sens. Environ. 232, 11309.
Windrim, L., Bryson, M., 2020. Detection, segmentation, and model fitting of individual tree stems from airborne laser scanning of forests using deep learning. Remote Sens.-Basel. 12.
Xi, Z., Hopkinson, C., Chasmer, L., 2018. Filtering stems and branches from terrestrial laser scanning point clouds using deep 3-D fully convolutional networks. Remote Sens.-Basel. 10.
Xi, Z., Hopkinson, C., Rood, S.B., Peddle, D.R., 2020. See the forest and the trees: Effective machine and deep learning algorithms for wood filtering and tree species classification from terrestrial laser scanning. ISPRS J. Photogramm. 168, 1–16.
Xu, T., Xu, L., Yang, B., Li, X., Yao, J., 2017. Terrestrial laser scanning intensity correction by piecewise fitting and overlap-driven adjustment. Remote Sens.-Basel. 9.
Yang, X., Strahler, A.H., Schaaf, C.B., Jupp, D.L.B., Yao, T., Zhao, F., Wang, Z., Culvenor, D.S., Newnham, G.J., Lovell, J.L., 2013. Three-dimensional forest reconstruction and structural parameter retrievals using a terrestrial full-waveform lidar instrument (Echidn (R)). Remote Sens. Environ. 135, 36–51.
Yao, T., Yang, X., Zhao, F., Wang, Z., Zhang, Q., Jupp, D., Lovell, J., Culvenor, D., Newnham, G., Ni-Meister, W., 2011. Measuring forest structure and biomass in New England forest stands using echidna ground-based lidar. Remote Sens. Environ. 115, 2965–2974.
Yu, X., Liang, X., Hyyppa, J., Kankare, V., Vastaranta, M., Holopainen, M., 2013. Stem biomass estimation based on stem reconstruction from terrestrial laser scanning point clouds. Remote Sens. Lett. 4, 344–353.
Zhang, J., Lin, X., Ning, X., 2013. SVM-based classification of segmented airborne lidar point clouds in urban areas. Remote Sens.-Basel. 5, 3749–3775.
Zhang, W., Wan, P., Wang, T., Cai, S., Chen, Y., Jin, X., Yan, G., 2019. A novel approach for the detection of standing tree stems from plot-level terrestrial laser scanning data. Remote Sens.-Basel. 11.
Zhang, Z., Liu, X., 2016. Support vector machines for tree species identification using lidar-derived structure and intensity variables. Geocarto Int. 2016, 364–378.
Zhao, F., Yang, X., Schull, M.A., Román-Colón, M.O., Yao, T., Wang, Z., Zhang, Q., Jupp, D.L.B., Lovell, J.L., Culvenor, D.S., 2011. Measuring effective leaf area index, foliage profile, and stand height in New England forest stands using a full-waveform ground-based lidar. Remote Sens. Environ. 115, 2954–2964.
Zhou, J., Wei, H., Zhou, G., Song, L., 2019. Separating leaf and wood points in terrestrial laser scanning data using multiple optimal scales. Sensors-Basel. 19.
Zhu, X., Skidmore, A.K., Wang, T., Liu, J., Darvishzadeh, R., Shi, Y., Premier, J., Heurich, M., 2018. Improving leaf area index (LAI) estimation by correcting for clumping and woody effects using terrestrial laser scanning. Agr. Forest Meteorol. 263, 276–286.